Measuring and modelling transpiration of pine and oak forest stands in a Mediterranean mountain area (Vallcebre, NE Spain)

TESI DOCTORAL

Rafael Poyatos López

2006

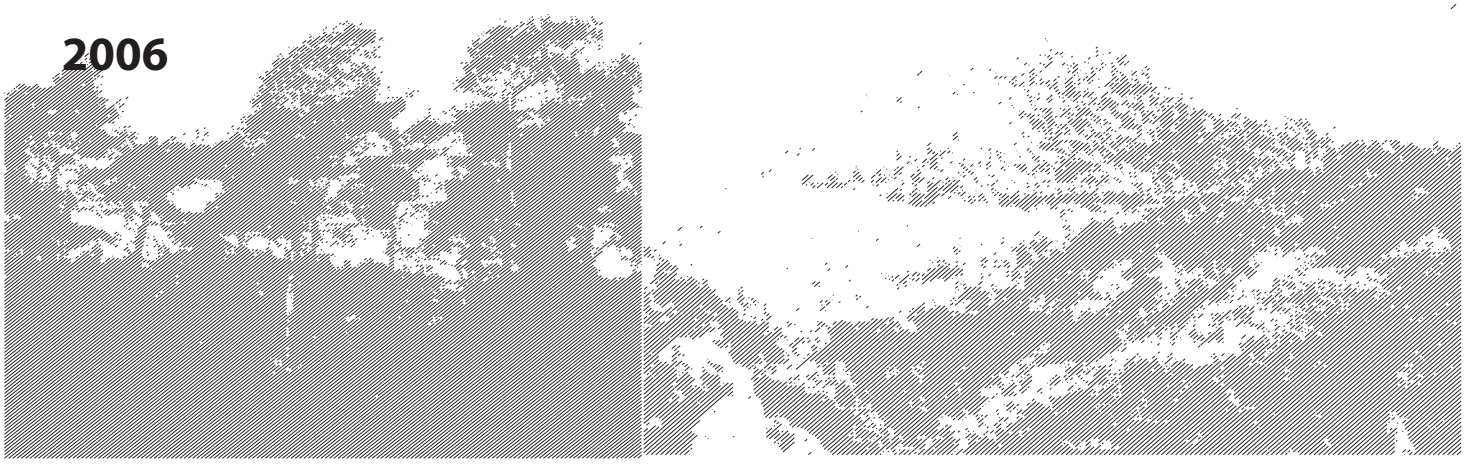

4. Parameterisation and application of a two-source evapotranspiration model in a Scots pine stand under Mediterranean mountain conditions

---

[1] Rafael Poyatos, [2] Luis Villagarcía, [3] Francisco Domingo, [4] Josep Piñol and [1] Pilar Llorens

In preparation for submission to *Agricultural and Forest Meteorology*.

Despite all the computations
You could just dance to a rock 'n ' roll station
And it was alright.

Rock & Roll, The Velvet Underground

[1] Institute of Earth Sciences 'Jaume Almera' (CSIC)

[2] Departamento de Sistemas Físicos, Químicos y Naturales. Universidad Pablo de Olavide.

[3] Estación Experimental de Zonas Áridas (CSIC).

[4] Centre de Recerca Ecològica i Aplicacions Forestals (CREAF), Universitat Autònoma de Barcelona

Abstract
Forest evapotranspiration has been the object of diverse modelling approaches in hydrology and ecophysiology, using representations of canopy structure and surface control of evaporation of varied complexity. In this paper we used a two-source evapotranspiration model to predict canopy transpiration (E_c) and soil evaporation (E_s) in a Scots pine under Mediterranean mountain conditions. Canopy stomatal conductance (G_s), obtained from stand scale sap flow, was modelled using a semiempirical Jarvis-type model, whereas soil resistance to evaporation was expressed as a function of superficial soil moisture. The evapotranspiration model was first used with a calibration of the G_s model on sap flow data obtained during the year 2004 using quantile regression techniques (boundary-line parameterisation).Validation using two more datasets (2003 and 2005) showed how the model tended to overpredict E_c under ample soil moisture conditions. Model performance with respect to daily values of E_c for the years 2003 and 2004 was within the usual range for this kind of models, but validation against data from the year 2005 showed a poor agreement with observations. Maximum modelled E_s rates were 0.7 mm day^{-1} with the ratio E_c/E_s being typically under 0.3 during the growing season. A Generalized Likelihood Uncertainty Estimation (GLUE) calibration was carried out using 2003 and 2004 data. The best parameter set in the GLUE analysis showed better overall performance than the boundary-line parametrisation. Parameters representing reference stomatal aperture and sensitivity to vapour pressure deficit (D) were the most relevant, whereas those controlling the response to soil moisture deficit ($SMD_{0\text{-}30}$) only appeared sensitive when calibration against 2003 data was done. Combinating calibration results from 2003 and 2004 showed how predictive uncertainty was reduced and the value of some parameters was constrained. Nevertheless, despite the exhaustive exploration of the parameter space in the GLUE analysis, the model continued to yield a poor performance for the year 2005, suggesting that the Jarvis algorithm cannot adequately simulate long-term E_c under the studied conditions.

Resum
L'evapotranspiració dels boscos ha estat objecte de diverses aproximacions en la modelització hidrològica i ecofisiològica, utilitzant representacions de l'estructura de la capçada i del control de l'evaporació de complexitat variable. En aquest article s'utilitza un model d'evapotranspiració de dues capes per tal de predir la transpiració de la capçada (E_c) i del sòl (E_s) en una pineda de pi roig en condicions de muntanya Mediterrània. La conductància estomàtica de la capçada (G_s), obtinguda a partir de les mesures de flux de saba a escala de cobert, fou simulada utilitzant un model semi-empíric de tipus *Jarvis*, mentre que la resistència del sòl a la evaporació s'expressà en funció de la humitat superficial d'aquest. El model d'evapotranspiració s'utilitzà en primer lloc calibrant el model de G_s amb les dades de flux de saba obtingudes durant l'any 2004 realitzant una parametrització per envolvents (*boundary-line parametrisation*) emprant tècniques de regressió de quantils. La validació amb els dos altres jocs de dades (2003 i 2005) mostrà que el model tendia a sobreestimar E_c en un ample rang de condicions d'humitat del sòl. Els resultats del model pel que fa als valors diaris de E_c per als anys 2003 i 2004 estaven dins d'un rang acceptable per aquests tipus de models, però la validació amb les dades de l'any 2005 mostrà poca concordança amb les observacions. Les taxes màximes d'E_s foren de 0.7 mm dia^{-1} amb una raó E_c/E_s normalment per sota de 0.3 durant el període de creixement. Una calibració de tipus GLUE (*Generalized Likelihood Uncertainty Estimation*) s'utilitzà per calibrar el model utilitzant les dades del 2003 i del 2004. El millor conjunt de paràmetres obtingut en l'anàlisi GLUE presentà millor resultats que la parametrització per envolvents. Els paràmetres representant l'obertura estomàtica i la sensibilitat al dèficit de pressió de vapor (D) foren els més rellevants, mentre que els que controlen la resposta al dèficit hídric del sòl ($SMD_{0\text{-}30}$) només resultaren sensibles quan es calibrà amb el joc de dades del 2003. La combinació dels resultats de les calibracions de 2003 i 2004 mostrà una reducció de la incertesa en la predicció i una restricció del rang d'alguns paràmetres.Tot i l'exhaustiva exploració de l'espai de paràmetres en l'anàlisi

GLUE, el model continuà simulant amb poca exactitud l'any 2005, suggerint que l'algoritme de Jarvis no és capaç de simular correctament la E_c a llarg termini en les condicions estudiades.

Introduction

Forest evapotranspiration constitutes an important fraction of total water loss from land surfaces into the atmosphere and therefore, adequate models of this process are needed for accurate predictions of water balance in forested watersheds. These models incorporate the active role of vegetation in regulating water vapour fluxes into the atmosphere, establishing a close link between disciplines such as hydrology, micrometeorology and ecophysiology.

Models of forest evapotranspiration usually combine some form of the Penman-Monteith equation (Monteith 1965) with a representation of the surface and aerodynamic controls in a resistance network (Huntingford et al. 1995; Raupach and Finnigan 1988). These models basically differ in the degree of detail in the physical representations of the canopy (the complexity of the resistance network) and the description of physiological regulation of transpiration by forest canopies.

When canopies are uniform and closed, spatially aggregated models ('big-leaf') often yields satisfactory results (Bernhofer et al. 1996). At the other end, multi-layer schemes offer more realistic descriptions of canopy structure of heterogeneous surfaces (Raupach and Finnigan 1988), but these approaches are computationally and data-intensive and become less appropiate as spatial scale increases (McNaughton and Jarvis 1991). A compromise between multi-layer and 'big-leaf' approaches are multiple-source interactive models, which allow the consideration of two (Shuttleworth and Wallace 1985) or more surfaces (Brenner and Incoll 1997) with different properties and distinct values of vapour pressure deficit. Furthermore, they include the interaction between overstory and understory fluxes and its consequences on within-canopy microclimate (Daamen and McNaughton 2000).

Whereas soil surface resistance depends mainly on soil physical properties and surface soil moisture (Wallace 1995) and is frequently modelled using simple relationships with topsoil water content (Camillo and Gurney 1986), complex empirical and semiempirical representations of plant surface resistance, are widely used within these model structures. Plant surface resistance is mainly determined by stomatal aperture, which can be modelled based solely on water relations (Jarvis 1976), or coupling transpiration and photosynthesis (Leuning 1995). Coupled models are preferred when the purpose is to model water vapour and CO_2 exchange between the canopy and the atmosphere (Hanson 2004). The Jarvis algorithm, although purely empirical has been shown to

represent adequately the underlying physiological processes of stomatal regulation in hydrological applications (Mackay et al. 2003a).

Canopy transpiration and soil evaporation measurements are commonly used to parameterise plant (Granier et al. 1996) and soil resistances (Domingo et al. 1999). Parameter optimisation of Jarvis-type models involves separate boundary-line analysis of canopy stomatal conductance (G_s) against the individual meteorological variables (Chambers et al. 1985). However, it has long been recognised that for soil-vegetation-atmosphere transfer models (Franks et al. 1997), and in general for environmental models (Beven and Freer 2001) many parameter sets will yield acceptable simulations. The Generalized Likelihood Uncertainty Estimation (GLUE) procedure was developed to deal with this equifinality problem (Beven and Binley 1992) . This methodology is also useful to investigate the sensitivity of the parameters within the model, the associated predictive uncertainty, and the effect of incorporating new data into the calibration procedure (Beven and Freer 2001).

In this study, carried out in a Scots pine (*Pinus sylvestris* L.) forest under Mediterranean mountain conditions, we used soil evaporation and sap flow measurements to parameterise the corresponding soil and plant surface resistances to evaporation in a two-layer interactive model scheme (Shuttleworth and Wallace 1985). The main aims of the study were (a) to parameterise soil and plant surface resistance in a two-layer interactive model (Shuttleworth and Wallace 1985) applied to a Mediterranean Scots pine stand, (b) to investigate the performance of the model under varying meteorological and soil moisture conditions, using independent sap flow datasets for validation, (c) to examine parameter sensitivity and predictive uncertainty using the GLUE procedure and (d) to compare the widely-used boundary-line calibration of Jarvis-type G_s models with the results from the GLUE calibration.

Table 1. List of relevant symbols in the model with their respective units.

Description	Symbol	Units
Canopy structure and aerodynamics		
Canopy height	h	m
Leaf Area Index	LAI	$m^2\ m^{-2}$
Plant Area Index	PAI	$m^2\ m^{-2}$
Roughness length	z_o	m
Radiation transfer and soil heat flux		
Above-canopy net radiation	R_n	$W\ m^{-2}$
Canopy net radiation	$R_{n,c}$	$W\ m^{-2}$
Below-canopy net radiation	$R_{n,s}$	$W\ m^{-2}$
Parameter describing leaf angle distribution	x	adimensional
Extinction coefficient for R_n	κ	adimensional
Sun zenith angle	θ_s	rad
Other meteorological variables		
Vapour pressure deficit at reference height	D_r	kPa
Vapour pressure at reference height	e_r	kPa

Table 1 (continued).

Air temperature at reference height	T_a	ºC
Wind speed at reference height	u	m s^{-1}
Resistance network		
Plant surface resistance	r^c_s	s m^{-1}
Soil surface resistance	r^s_s	s m^{-1}
Plant aerodynamic resistance	r^c_a	s m^{-1}
Soil aerodynamic resistance	r^s_a	s m^{-1}
Resistance between reference height and effective source/sink height	r^a_a	s m^{-1}
Parameters of the G_s model		
Canopy stomatal conductance	G_s	mm s^{-1}
Reference conductance at 1 kPa	$G_{s,ref}$	mm s^{-1}
Absolute sensitivity of G_s to ln D	m	mm s^{-1} ln kPa^{-1}
R_n at half-saturation of G_s	$R_{0.5}$	W m^{-2}
Threshold of G_s reduction with SMD_{0-30}	s	
Fraction of G_s when SMD_{0-30}=1	f_o	
Time optimum for G_s	t_{opt}	hours
Minimum time for G_s	t_{min}	hours
Maximum time for G_s	t_{max}	hours
Optimum air temperature for G_s	T_{opt}	ºC
Minimum air temperature for G_s	T_{min}	ºC
Maximum air temperature for G_s	T_{max}	ºC
Soil parameters		
Soil moisture (0-30 cm)	θ_{0-30}	cm^3 cm^{-3}
Soil moisture deficit (0-30 cm)	SMD_{0-30}	adimensional
Soil moisture deficit (30-60 cm)	SMD_{30-60}	adimensional
Soil moisture 0-15 cm	θ_{0-15}	cm^3 cm^{-3}
Soil moisture (0-15 cm) at field capacity	$\theta_{0-15,FC}$	cm^3 cm^{-3}
Parameter of soil surface resistance equation	b_1	s m^{-1}
Parameter of soil surface resistance equation	b_2	adimensional
Saturated vapour pressure at soil temperature	e_{Ts}^*	kPa
Other		
Canopy transpiration	E_c	mm s^{-1}, mm day^{-1}
Soil evaporation	E_s	mm s^{-1}, mm day^{-1}
Model efficiency	E_f	adimensional

Material and methods

Site and Stand characteristics

The experimental plot is part of the Vallcebre research area (42º 12′ N, 1º 49′ E), located in the Eastern Pyrenees (NE Spain). Climate is sub-Mediterranean, with an average air temperature of 7.3 ºC (measured at 1440 m.a.s.l.) and 924 mm of annual rainfall (Gallart et al. 2002). The present landscape is mainly a mosaic of mesophilous grassland of the *Aphyllantion* type and patches of Scots pine, which colonised old agricultural terraces after their abandonment (Poyatos et al. 2003).

The studied plot is located in a rather young stand (the oldest trees are about 60 years old) overgrowing an abandoned terraced slope, at an elevation of *ca.* 1260 m.a.s.l. The understorey is scarce, mainly scattered *Buxus sempervirens* L. shrubs, and a discontinuous herb layer. Mudstone and sandstone are the principal underlying lithologies, originating sandy-loam soils about 65 cm deep (Rubio, personal communication). Biometric characteristics of the stand are summarized in Chapter 1.

Meteorological, soil moisture and sap flow measurements

Above-canopy meteorology, soil moisture and sap flow by the heat dissipation method (Granier 1985) were measured continuously between June 2003 and August 2005. For details of meteorological, soil moisture and sap flow instrumentation see Chapter 1. Additional measurements of soil moisture between 30 and 60 cm depth were taken on a weekly basis, at two locations in the plot, using the TDR technique. Upscaling of sap flow measurements in individual trees was done according to the measured radial patterns in each particular tree (see Chapters 2 and 3 for details).
Below-canopy net radiation ($R_{n,s}$) and soil heat flux (G) were also measured during July and August of year 2005 to parametrise the radiative transfer within the canopy. We obtained the estimates of $R_{n,s}$ by averaging the measurements from three net radiometers (Q7, REBS, Seattle, WA, USA) randomly placed above the forest soil. Four soil heat flux plates (HFT-3, REBS, Seattle, WA, USA) were also installed to measure soil heat flux at a depth of 0.08 m, and above each plate, a set of soil thermocouples (TCAV, Campbell Scientific) inserted at 0.02 and 0.06 m depth, measured the average temperature of the soil layer above the plates. Consecutive differences in soil temperature, together with soil moisture estimates for the topsoil (see next section) and bulk density of the soil, were used to calculate the energy stored above the heat flux plates (Massman 1992), which was added to the flux measured by the plates to obtain total soil heat flux. A general description of the meteorology during the period of study can be found in chapter 5.

Soil evaporation measurements

Soil evaporation meaurements were carried out following the recommendations by Daamen et al. (1993). Six PVC cylinders of 11.8 cm in diameter and 15 cm depth were randomly installed in the forest soil (lysimeter cases). For each measurement date, a set of 4-6 soil cores were extracted by hammering a PVC tube (diameter 10.8 cm, 15 cm long) into the soil in a nearby location. These lysimeters were sealed with a PVC cap and then inserted into the lysimeter cases, covering the top of the lysimeter with a plastic mesh to

avoid measurement errors due to litterfall. The lysimeters were weighed in the morning between 7:00-8:00 solar time, and then in the evening (18:00-19:00 solar time). Soil evaporation rate was then calculated from the difference in weight divided by the time between measurements.

Model parameterisation

We refer to the appendix for the basics of the Shuttleworth and Wallace (1985) evapotranspiration model, but in this section we will detail the modifications in the radiative transfer and resistance parameterisation that will be included in this particular application, and the different datasets used for model calibration.

A micrometeorological dataset obtained during July 2005 was used to parameterise radiative transfer within the canopy. Stand-scale sap flow, meteorological and soil moisture data measured during the year 2004 (Table 2) were used to parameterise canopy surface resistance (r_s^c) and soil evaporation measurements, as described above, were used to parameterise soil surface resistance (r_s^s).

Table 2. Characteristics of the datasets used in the calibration and validation stages. One-year periods are shown for better comparison of meteorological conditions across years.

Year	Period (days)	Average D_r (kPa)	Rainfall (mm)	$\theta_{0\text{-}30}$ (cm^3cm^{-3})	Calibration procedures: Boundary-line	Calibration procedures: GLUE
2003	205-365	0.68	433	0.24	Validation	Calibration*,†
2004	1-362	0.56	644	0.23	Calibration*	Calibration*
2005	1-212	0.77	312	0.19	Validation	Validation
Equal-length periods						
2003-2004	July 2003-June 2004	0.53	824	0.24	-	-
2004-2005	July 2003-June 2004	0.77	566	0.19	-	-

* The model has been validated separately for each year and therefore calibration data has also been used for validation.

† Dataset used to update likelihoods obtained when the model was constrained with 2004 data.

Parameterisation of radiation transfer and soil heat flux

Above-canopy net radiation (R_n) was partitioned between canopy (R_n^c) and soil (R_n^s) according to:

$$R_n^c = R_n - R_n^s \quad (1)$$

and the penetration of net radiation through the canopy was modelled according to Lambert-Beer's law

$$R_n^s = R_n \exp(-\kappa \cdot f(\Theta_s, x) \cdot PAI) \quad (2)$$

Where the function *f* accounted for the variation of the extinction coefficient with sun zenith angle (Θ_s) and leaf angle distribution (*x*), κ is the extinction coefficient for net raditation and PAI is plant area index. We assumed an elliptical leaf angle distribution,

$$f(\theta_s, x) = \frac{[(x^2 + \tan^2 \Theta_s)^{0.5}]}{x + 1.774(x + 1.182)^{-0.733}} \quad (3)$$

with the value *x*=3.33 obtained from previous measurements in nearby stands (Llorens and Gallart 2000) and a maximum plant area index of 2.8, which was obtained by adding to LAI a fixed amount corresponding to branch fraction (Llorens and Gallart 2000) . The value of κ was obtained using measured $R_{n,s}$ and R_n and inverting the model described above for a period with clear skies (days 215-218, August 2005).

A preliminary analysis of the correlation between measured soil heat flux (*G*) and radiation reaching the soil showed that *G* was better correlated with $R_{n,s}$ at t_{-4}, that is, soil heat flux lagged one hour behind radiative input at the forest soil. Therefore, we used this 1h-lagged $R_{n,s}$, soil water content in the first 15 cm ($\theta_{0\text{-}15}$) and air temperature as independent variables to predict soil heat flux using a multiple regression model fitted to measured data (days 214-221, August 2005).

Parameterisation of soil surface resistance

We calculated the soil surface resistance to evaporation r_s^s as:

$$r_s^s = \frac{(0.622\rho / P)(e_{Ts}^* - e_r)}{E_s} - r_a^s \quad (4)$$

Where ρ_a is air density (kg m^{-3}), *P* is atmospheric pressure in kPa, e_{Ts}^* is saturated vapour pressure in soil pore space, e_r is vapour pressure at the reference height, E_s is soil evaporation (kg m^{-2} s^{-1}) and r_a^s is aerodynamic resistance (s m^{-1}). We used soil evaporation measured with microlysimeters to calculate r_s^s and then relate its value to the soil moisture conditions of the plot.

Overall, we obtained fifteen estimates of r_s^s in four measurement dates along the year 2005 (19 and 20th of May, 4th of August and 24th August). Soil surface resistance estimated for each lysimeter and measuring date was related to volumetric soil moisture of the lysimeter ($\theta_{0\text{-}15}$) fitting a power relationship,

$$r_s^s = b_1 \left(\frac{\theta_{0-15}}{\theta_{0-15,FC}} \right)^{b_2} \quad (5)$$

Where $\theta_{0\text{-}15,FC}$ is the corresponding value of soil moisture at field capacity ($\theta_{0\text{-}15,FC}$ = 0.35 cm^3 cm^{-3}, C.Rubio, personal communication).

A linear relationship between the average soil moisture of the plot in the upper 30 cm ($\theta_{0\text{-}30}$) and soil moisture in the lysimeters was fitted in order to directly relate the value of soil surface resistance to the average soil moisture measured continuously.

Parameterisation of canopy resistance

Canopy surface resistance (r_s^c) is defined in the model as

$$r^c{}_s = \frac{1}{G_s LAI} \quad (6)$$

Where G_s is canopy stomatal conductance and LAI is stand leaf area index (see Chapter 2 for details on LAI estimation). Leaf area index seasonal variation was assessed from observations of the onset of leaf elongation in late spring and leaf senescence in autumn, and assuming that a fixed fraction of maximum LAI remains throughout late autumn, winter and early spring (Beadle et al. 1982).

Canopy stomatal conductance was first calculated from stand-scaled sap flow measurements and meteorological data, using the inversion of the Penman-Monteith equation for well coupled canopies (Whitehead and Jarvis 1981) and assuming no capacitance effects. Then, G_s was parameterised using data with D_r>0.6 kPa to minimise the measurements errors in G_s (Ewers and Oren 2000), as a function of the main meteorological variables (Jarvis 1976):

$$G_s = G_{s,\max}(D) f_1(R_n) f_2(T) f_3(SMD_{0-30}) f_4(t) \quad (7)$$

Maximum conductance $G_{s,max}$ was constrained by a series of functions which depend on single environmental variables: R_n, air temperature (T), soil moisture deficit ($SMD_{0\text{-}30}$) and time of day (t). Soil moisture deficit in the upper 30 cm ($SMD_{0\text{-}30}$) was calculated using $\theta_{0\text{-}30}$ as described in Granier and Loustau (1994) (see also Chapter 2).

Parameterisation of individual constraint functions of a given variable in G_s multiplicative models is usually carried out by selecting different subsets of data where the rest of the variables present in the model are considered non-limiting for G_s. However we used a sequential calibration procedure using boundary-line analysis (Granier et al. 2000; Lagergren and Lindroth 2002). We began parametrising the response of G_s to D by means of a boundary-line analysis, using the quantile regression of the 99th quantile for that purpose (procedure rq, R Statistical Software v. 2.0.1; see Chapters 1 and 5 for more detailed descriptions of the procedure). The model suggested by Oren et al. (1999) was adopted:

$$G_{s,\max} = G_{s,ref} - m \cdot \ln D \quad (8)$$

We selected the intercept and slope of the 99th quantile fit as representative of the relationship between G_s and ln D at optimal conditions, and therefore of the coefficients $G_{s,ref}$ and m, respectively. After estimating $G_{s,max}$ we looked for a relationship between the ratio of the measured conductance and $G_{s,max}$ and R_n. If this ratio was greater than 2, the value was omitted from the analysis. Nonlinear quantile regression (procedure nlrq in the quantreg package, R Statistical Software v.2.0.1) was used in this case to find the fit for the 99th quantile of the equation

$$f_1(R_n) = \frac{R_n}{R_{n,0.5} + R_n} \tag{9}$$

Where the parameter $R_{n,0.5}$ represents the value of R_n at which $f(R_n)$ is 0.5.

Based on the prior information on the reduction of conductance with soil moisture in *P.sylvestris* (Irvine et al. 1998; Lagergren and Lindroth 2002) we established a soil moisture function with two parameters: s, defining the threshold beyond which soil water supply limits transpiration and f_0, meaning the fraction of transpiration that is still sustained when $SMD_{0\text{-}30}$=0:

$$\begin{aligned} &SMD_{0-30} < s \Rightarrow f_2(SMD_{0-30}) = 1 \\ &s < SMD_{0-30} < 1 \Rightarrow f_2(SMD_{0-30}) = \left(\frac{f_0 - 1}{1 - s}\right) SMD_{0-30} + \left(\frac{1 - sf_0}{1 - s}\right) \end{aligned} \tag{10}$$

The resulting relationship equals 1 when $SMD_{0\text{-}30}<s$, reduces to f_0 when $SMD_{0\text{-}30}$=0 and shows a linear decrease when $s < SMD_{0\text{-}30} < f_0$. We chose the value of the parameters (s=0.6, f_0=0.4) according to previous studies in the same plot (Poyatos et al. 2005).

The constraint function for temperature was found in an analogous way to $f(R_n)$ (i.e. relating the ratio $G_s/(G_{s,max}(D)\cdot f_1(R_n)\cdot f_2(SMD_{0\text{-}30}))$ to air temperature, using a quadratic function with T_{min}, T_{max} and T_{opt} being minimum, maximum and optimum temperatures, respectively

$$f_3(T) = \frac{(T - T_{\min})}{(T_{opt} - T_{\min})} \cdot \frac{(T_{\max} - T)}{(T_{\max} - T_{opt})} \tag{11}$$

Finally as an additional dependence of G_s with time of day was observed in previous analysis, a quadratic function equivalent to that of temperature was included to correct for this effect, where a time optimum t_{opt} was also found using nonlinear quantile regression:

$$f_4(t) = \frac{(t - t_{\min})}{(t_{opt} - t_{\min})} \cdot \frac{(t_{\max} - t)}{(t_{\max} - t_{opt})} \tag{12}$$

Parameterisation of aerodynamic resistances

Three aerodynamic resistances are involved in the model, r^c_a and r^s_a, canopy and soil aerodynamic resistances, respectively and the resistance between reference height and the effective source/sink height, r^a_a. All of them were calculated assuming a logarithmic wind profile, K-theory for eddy and characteristic leaf dimensions and canopy structure for Scots pine (Shuttleworth and Gurney 1990). A mode detailed description of the resistance network of this model can be found in Iritz et al.(1999).

Parameter conditioning using Generalised Likelihood Uncertainty Estimation (GLUE)

We carried out an alternative calibration using the GLUE methodology, which do not consider the existence of a global optimum parameter set, due to the uncertainties present both in models and experimental data, and the inherent complexity of high dimensional parameter spaces (Beven and Binley 1992). Instead, GLUE analysis retains, from a large sample of parameter sets, the models which are considered to be acceptable simulators of our system (or 'behavioural').

Thirty thousand Monte Carlo simulations were performed using parameters randomly sampled from uniform distributions with ranges established according to previous experience and preliminar Monte Carlo runs. All the parameters in the G_s submodel and canopy roughness length (z_0), which affects aerodynamic resistance, were included in the GLUE analysis (Table 3). In addition to the initial calibration data (2004), the GLUE procedure was also carried out using data from another period in 2003 (Table 2). Each simulation was performed using the available meteorological data and the resulting simulated E_c was compared to experimentally measured E_c from sap flow. We computed model efficiency (E_f) (Nash and Sutcliffe 1970) for each run and used it as a likelihood measure:

$$L(\Theta_j \mid \mathrm{Y}) = 1 - \frac{\sum_{\mathrm{j=1}}^{\mathrm{N}} (O_{\mathrm{i}} - P_i)^2}{\sum_{\mathrm{j=1}}^{\mathrm{N}} (O_i - \overline{O})^2} \qquad (13)$$

$L(\Theta_j|Y)$ is the likelihood measure for the *j*th parameter set (Θ_j) conditioned on the observations Y. The right hand-side of the equation equals model efficiency, which equals 1 for a perfect fit, with O_i and P_i being observed and predicted values of E_c at the *i*th time step and $\overline{O}$ the mean of observed values. Model efficiency, whose maximum value equals 1 for a perfect fit, was calculated both at the 15-min step and also on a daily basis. Models

with E_f<0 were rejected for further analysis, as negative efficiencies are no better than a mean of the data (Nash and Sutcliffe 1970).

Table 3. Range of parameters and the distribution from which they were sampled in the GLUE analysis

Parameter	Distribution	Minimum	Maximum	Units
$G_{s,ref}$	Uniform	2.0	10.0	mm s^{-1}
m	Uniform	1.0	10.0	mm s^{-1} ln kPa^{-1}
$R_{n,0.5}$	Uniform	0	500	W m^{-2}
s	Uniform	0.2	1	Adimensional
f_0	Uniform	0	1	Adimensional
t_{opt}	Uniform	4	20	hour (decimal)
T_{opt}	Uniform	5	35	ºC
z_o	Uniform	1.0	6.0	m

Scatter plots displaying E_f against each parameter's value were examined to infer the characteristics of the parameter space with regard to model performance. Two different efficiency thresholds for behavioural models were considered for the instantaneous and daily cases (0.5 and 0.75 respectively). Then, cumulative likelihood distributions of the parameters for behavioural and non-behavioural models were compared to assess the sensitivity of each parameter. If uniform distributions were obtained (straight lines), the parameter was considered to be insensitive to the likelihood measure chosen.

Predictive uncertainty bounds were estimated at each time step by ranking the outputs from behavioural models according to their likelihood weights, and deriving a cumulative distribution (Franks and Beven 1997). Likelihood weights had been previously obtained by rescaling the efficiencies of the behavioural models in order that their sum was 1. We chose the 5% and 95% quantiles of the resulting distribution to represent predictive uncertainty related to model calibration with 2004 and 2003 data.

The GLUE methodology allows the combination of likelihoods when more data becomes available. In this study, the initial parameter conditioning on 2004 data was updated with the results from the GLUE analyisis for 2003, making use of the Bayes theorem to combine both likelihoods:

$$L(\Theta_j \mid \mathrm{Y}) = L(Y \mid \Theta_j) L_0(\Theta_j)/\mathrm{C} \qquad (14)$$

Where $L_0(\Theta_j)$ is a prior likelihood measure for the parameter set Θ_j, $L(Y|\Theta_j)$ is the likelihood measure obtained when conditioning on the new data set, $L(\Theta_j|Y)$ is the posterior likelihood after updating, and C is a scaling constant. This principle was also applied when carrying out the individual GLUE analysis, but as uniform distributions for parameters were assumed, $L_0(\Theta_i)$ would have been constant and equation 14 would have yielded the same posterior as equation 13. In this way, if a parameter set performed badly in one of the calibration periods (i.e. it was non-behavioural), the combined likelihood yielded a value of zero.

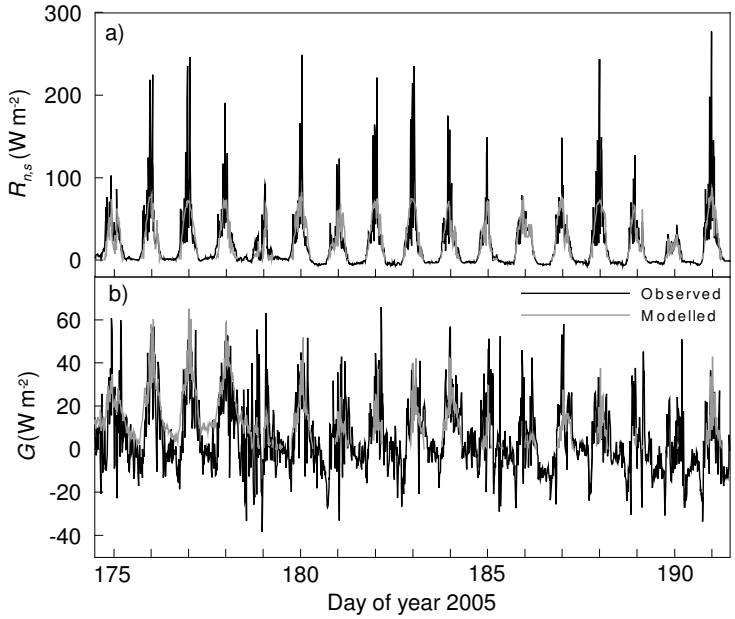

Figure. 1. Modelled and measured (a) Net radiation below the canopy ($R_{n,s}$) and (b) soil heat flux (G).

Results

Radiative transfer

The value of the extinction coefficient κ obtained from the inversion of the radiation transfer submodel was *ca.* 0.9, yielding an acceptable simulation of the overall diurnal course of net radiation within the forest. However, this approach could not reproduce the radiation peaks in the observations, which approached 250 W m^{-2} in some occasions (Fig.1). These differences had little impact on aggregated fluxes at the daily level.

Soil heat flux was modelled acording to the obtained multiple regression fit (G=0.19*$R_{n,s}$(t-4)+2.61*T+188.51θ_{15}; R^2=0.58;N=480). Again, the peaky dynamics of G could not be simulated, but the overall daily dynamics, which ranged between -40 and 60 W m^{-2} was appropiately represented (Fig.1).

Optimisation of soil and canopy resistances

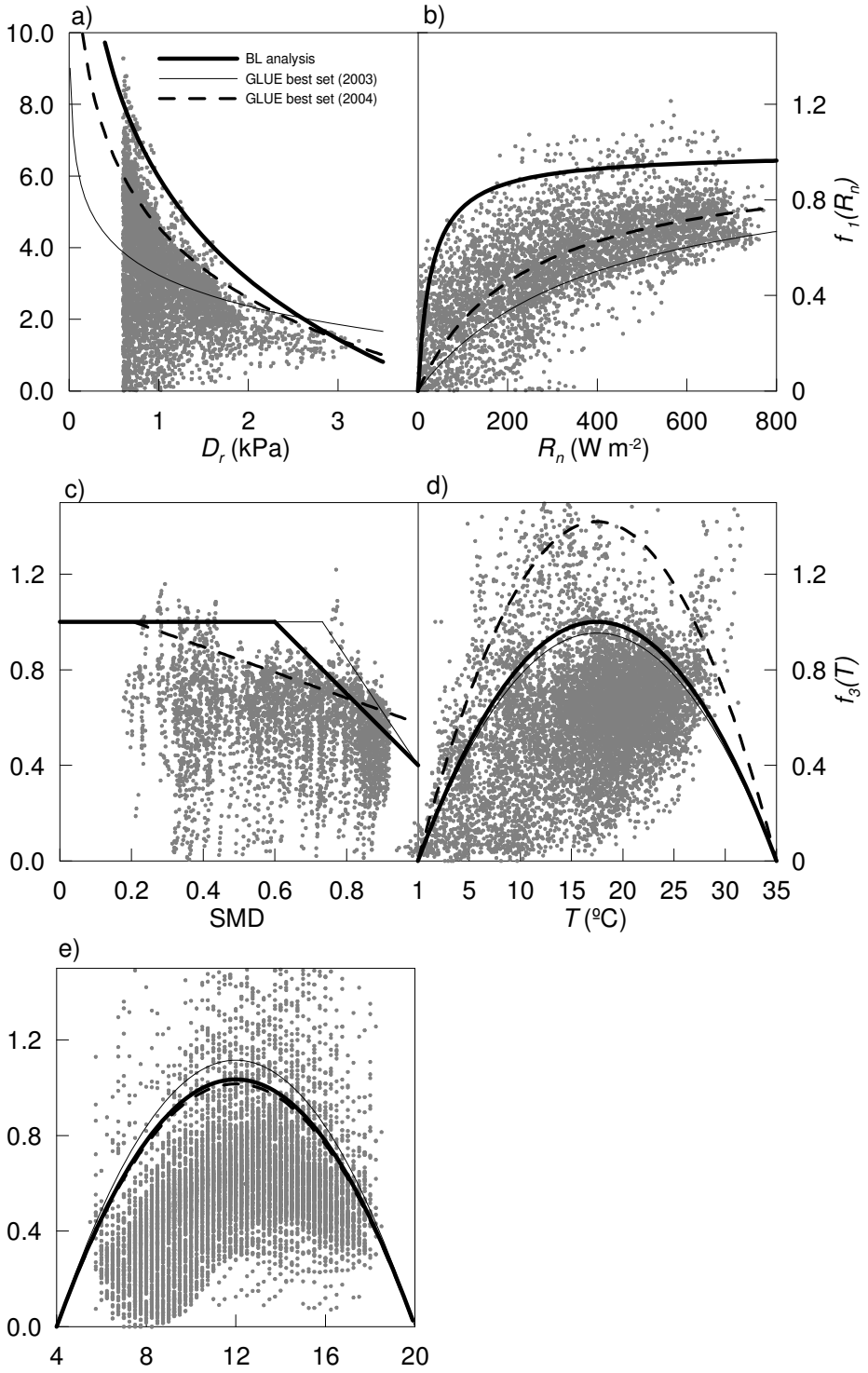

Figure 2. Results of the canopy stomatal conductance parameterisation by boundary-line analysis, showing the resulting functions (thick lines) and the data points used to fit them. The best parameter sets obtained in the GLUE parameter conditioning on 2004 data (dashed lines) and 2003 data (thin lines) are also shown.

Soil evaporation measurements used for parametrising soil surface resistance were always below 0.15 mm day^{-1}. The value of r_s^s was related to soil moisture at the top 15 cm, relative to water content at field capacity, using a potential function (Eq. 5) with coefficients b_1=8.74 and b_2=-2.55 (R^2=0.43, N=14, P=0.011).

With respect to canopy stomatal conductance, the boundary line analysis results showed that G_s decreased strongly with D_r, increased very rapidly for low values of radiation and achieved its temperature and time optimums halfway between the considered minimum and maximum temperatures and time of day, respectively (Fig. 2). All the constraint functions in the Jarvis model showed maximum values close to unity.

Validation of the optimised model

The relationship between measured and observed values of instantaneous E_c varied across years (Fig. 3), with slopes significantly different from unity in all cases and positive intercepts (Table 5). Model performance was specially poor for the year 2005, both at the 15-min and daily time-scales.

We examined diurnal simulations under different evaporative demand and soil moisture conditions (Figs 4). The model overestimated E_c when SMD_{0-30} was low and D_r was below 2 kPa during a period in the summer of 2004 (Fig. 4b). Under conditions of high D_r and SMD_{0-30}, model overestimation was less marked, although when high D_r's were reached (up to 4 kPa), the predicted values of E_c declined rapidly and did not track the diurnal course of the observations (Fig. 4a). For a period with varying soil moisture and evaporative demand conditions during the year 2005, simulations and observed data were in close agreement only when SMD_{0-30} was high and considerable overestimation was found again when SMD_{0-30} was low (Fig. 4c). Model residuals decreased with D_r and T at low to intermediate values of these variables, but then increased at higher D_r and T (data not shown). We did not find any relationship between model residuals and SMD including deeper soil layers (0-60 cm) obtained from weekly TDR measurements (data not shown).

Aggregated daily E_c was generally overestimated by the model, especially during the year 2005 (Figs. 5,6), with E_f showing a negative value (Table 5). Maximum soil evaporation rates were estimated at less than 0.7 mm day^{-1}, although values between 0.1 and 0.5 mm day^{-1} were the most frequent (Fig. 6). On a daily basis, the ratio between modelled E_s and measured E_c was below 0.3 for almost 80% of the days during the growing season (days 140-300), but this changed for non-growing season days, with only a 40% of the days with E_s/E_c fractions below 0.3.

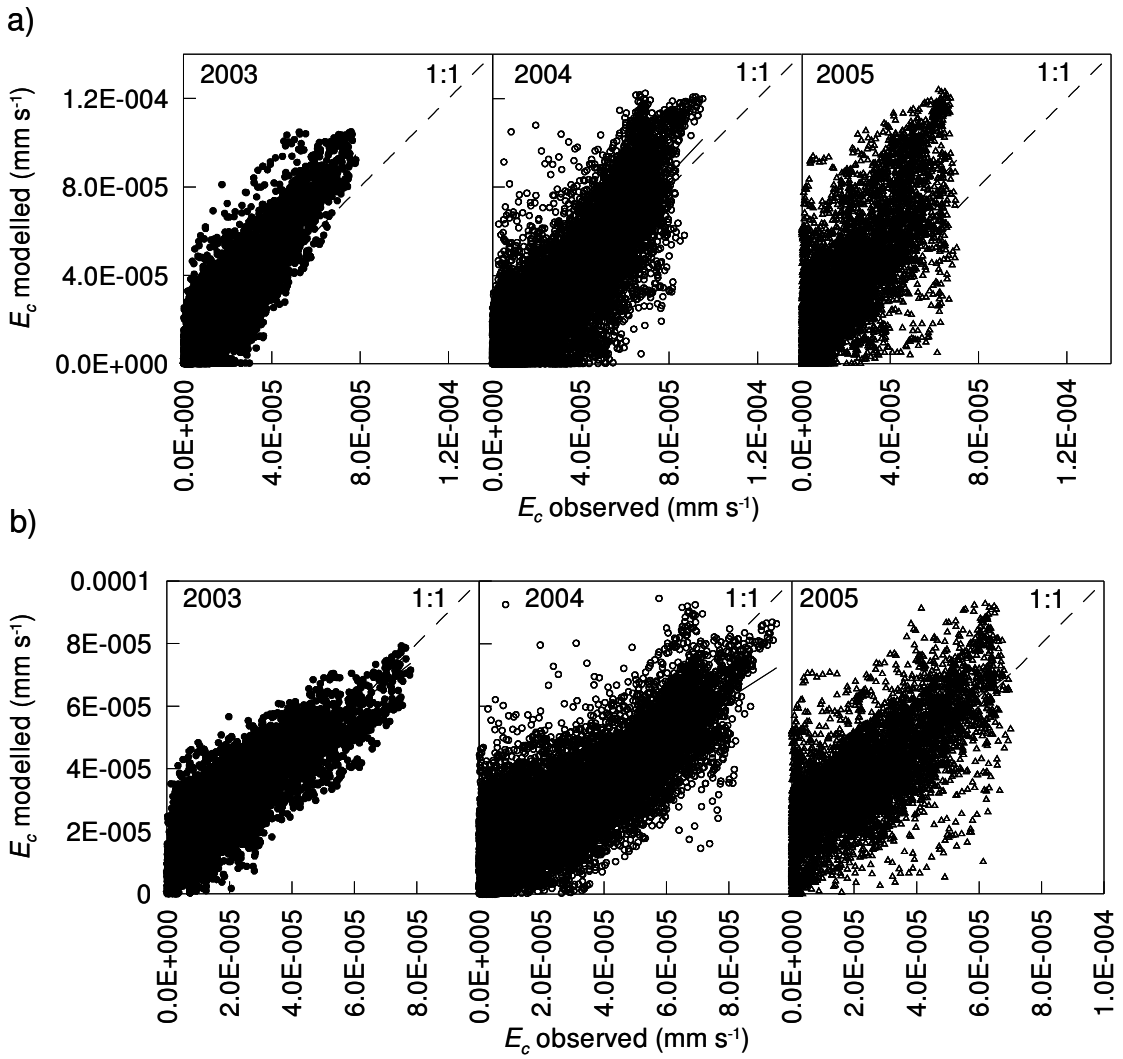

Figure 3. Observed and modelled E_c, with (a) the parameterisation obtained from the boundary line analysis and (b) the best parameter set obtained in the GLUE analysis with 2004 data. Fitting results in table 4.

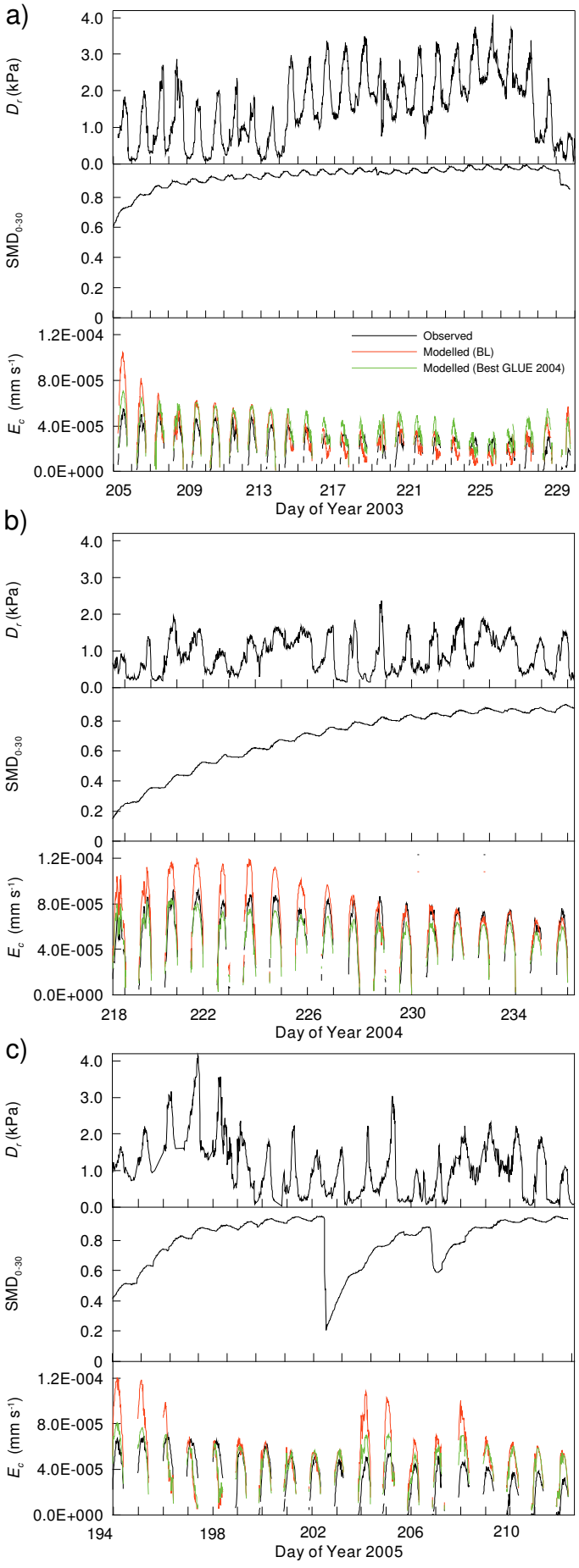

Figure 4. Observed and modelled Ec rates during three periods with varying soil moisture deficit and vapour pressure deficit conditions.

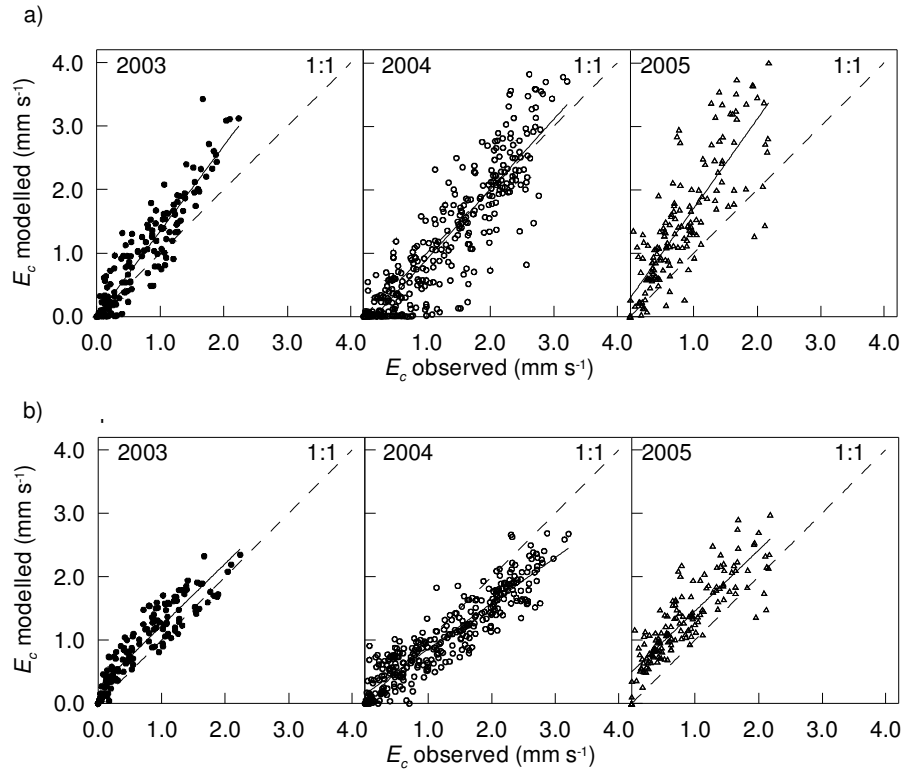

Figure 5. Oberved and modelled values of daily canopy transpiration (E_c) for each year during the measuring period, obtained with the boundary-line parameterisation (a) or the best parameter set in the GLUE analysis with data from the year 2004. Fitting results in table 4.

GLUE analysis:parameter space

For the year 2004, 15% of the simulations (more than 4500 parameter sets) had positive efficiencies when calculated at the 15-min level, but this number doubled (more than 10000 models) when daily efficiencies were considered. Maximum model efficiencies were greater when calculations of model performance were done at the daily time scale than for the instantaneous values (*ca.* 0.65 and 0.86, respectively). However, plots of parameter values against E_f calculated at the daily level showed very similar patterns to plots with E_f calculated at the 15-min level. Given this similarity between results at the 15-min and daily time scales, further analysis and discussion will be based on daily likelihoods.

The boundary-line parameterisation of the G_s model yielded worse results in terms of model efficiency than the best parameter set obtained in the GLUE calibration with data from the year 2004 (Table 5). Using this parameter set, simulated values did not overestimate E_c so much as the model with the boundary-line parameterisation (Fig. 4, 5). However, the resulting functions from the best parameter sets for the two conditioning periods (2004 and 2003) did not represent the envelope relationships of G_s against the individual variables in the G_s model (Fig. 1).

Table 4. Parameter values for the optimised model using the boundary-line technique and results for the best parameters sets from GLUE analysis for 2003 and 2004 data .

	$G_{s,ref}$	m	$R_{n,0.5}$	s	f_0	t_{opt}	T_{opt}	z_o
Optimised Model	5.96	4.11	30.00	0.60	0.4	10.52	17.0	3.60
GLUE (2004)	4.56	2.84	239.39	0.21	0.575	13.03	7.98	3.19
GLUE (2003)	3.23	1.25	398.36	0.73	0.40	14.58	17.93	3.34

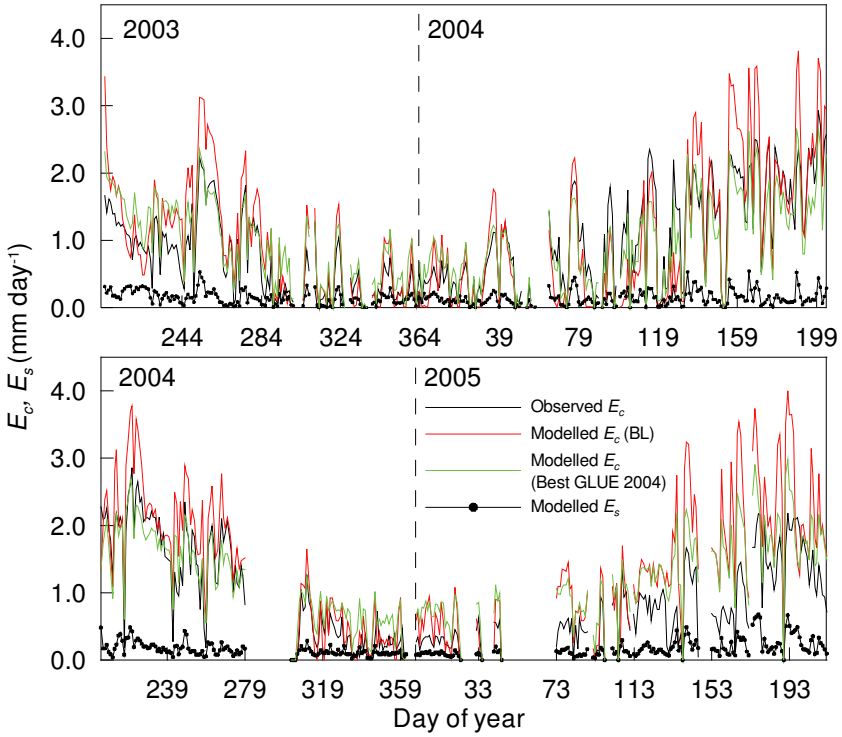

Figure 6. Time series of modelled and observed canopy transpiration (E_c) and modelled soil evaporation (E_s) during the whole study period. Modelled results for with the boundary-layer (BL) parametrisation and the best parameter set obtained in the GLUE calibration are shown.

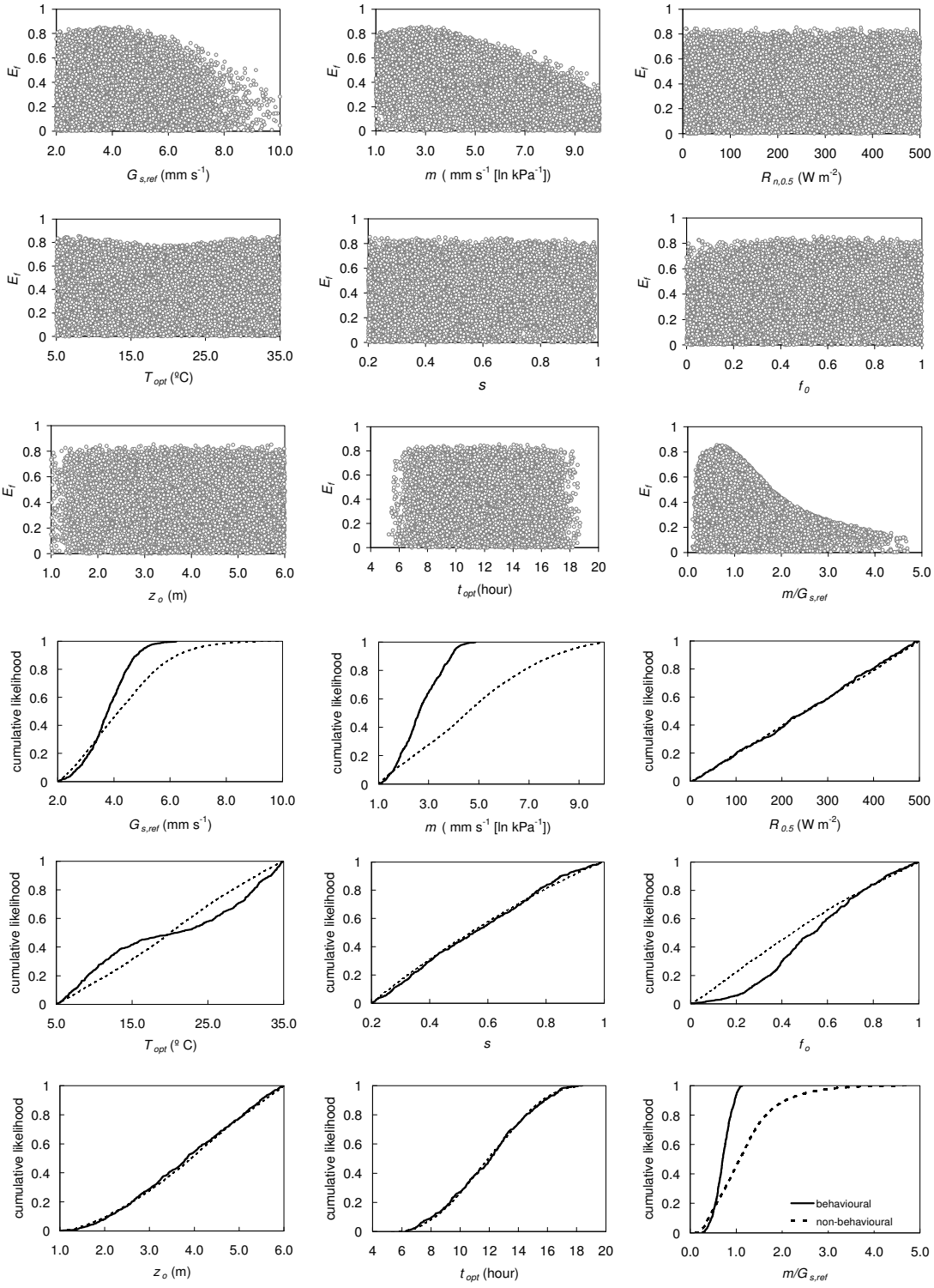

Figure 7. Parameter conditioning of the evapotranspiration model with sap flow data from year 2004 after 30,000 Monte Carlo realisations. (a) Plot of daily efficiency against parameter values included in the GLUE analysis (Table 2). Only simulations with E_f >0 are shown. (b) Cumulative likelihood distribution of the parameters, for behavioural (E_f>0.75) and non-behavioural models (E_f<0.75).

The range of the parameters $G_{s,ref}$ and m were noticeably constrained by the 2004 calibration data (Fig. 7a), as efficiency peaked at values of $G_{s,ref}$ about 4.5 mm s^{-1} and values of m of about 3.0 mm s^{-1} ln kPa^{-1}. The derived value of relative sensitivity of G_s to ln

D ($m/G_{s,ref}$) was likewise constrained at values lower than unity. For the rest of parameters, behavioural models were found across the whole sampled range (Fig. 7a). Differences in the cumulative distributions between behavioural (525 parameter sets in total) and non-behavioural models were clear for $G_{s,ref}$ and m, and also evident for T_{opt} and f_0 (Fig. 7b). Values of T_{opt} in the central part of the sampled range (15-25 ºC) were less probable than values at the extremes, and for f_0, values were mostly between 0.3 and 0.9. Remarkably, the parameters controlling the response to radiation and the threshold for reduction due to soil moisture deficits ($R_{n,0.5}$ and s) showed identical, almost uniform distributions for behavioural and non-behavioural sets (Fig. 7b).

Substantial differences were found when the model was constrained against 2003 data (Fig. 8), beginning with the number of behavioural models (160 parameter sets), which was much lower than in the previous GLUE exercise for the year 2004. The scatter plots showed that positive model efficiencies were less frequent at large values of $G_{s,ref}$ and m ($G_{s,ref} > 6.0$ and $m > 5.0$) (Fig. 8a). Contrarily to what occurred when conditioning on 2004 data, parameter sets with high E_f were found with T_{opt} values around the middle of the chosen parameter range. This was reflected in the narrower interquartilic range for T_{opt} when the model was conditioned on 2003 data (Fig. 9).

The two parameters defining the response of G_s to soil moisture deficit were more sensitive when calibrating against 2003 data. Only the ranges of $G_{s,ref}$, m, and to a lesser extent, f_0, changed appreciably with the data period used for conditioning (Fig. 9). The interquartilic ranges of the parameters in the models retained after updating the 2004 calibration with 2003 data, showed how $m/G_{s,ref}$ was constrained around 0.6, and s and f_0 were centered around 0.6 and 0.45, respectively (Fig. 9).

We examined the interactions between pairs of parameters in the behavioural sets obtained with 2003 and 2004 data (Fig. 10). For 2004, it can be seen that at a given value of $m/G_{s,ref}$ between 0.6-0.8, higher E_f concentrated in a wide range of s and f_0. As we have shown earlier, higher efficiencies lie in the extreme values of T_{opt}. If behavioural models conditioned on 2003 data are considered, the regions with the best model performance could be clearly delimited.

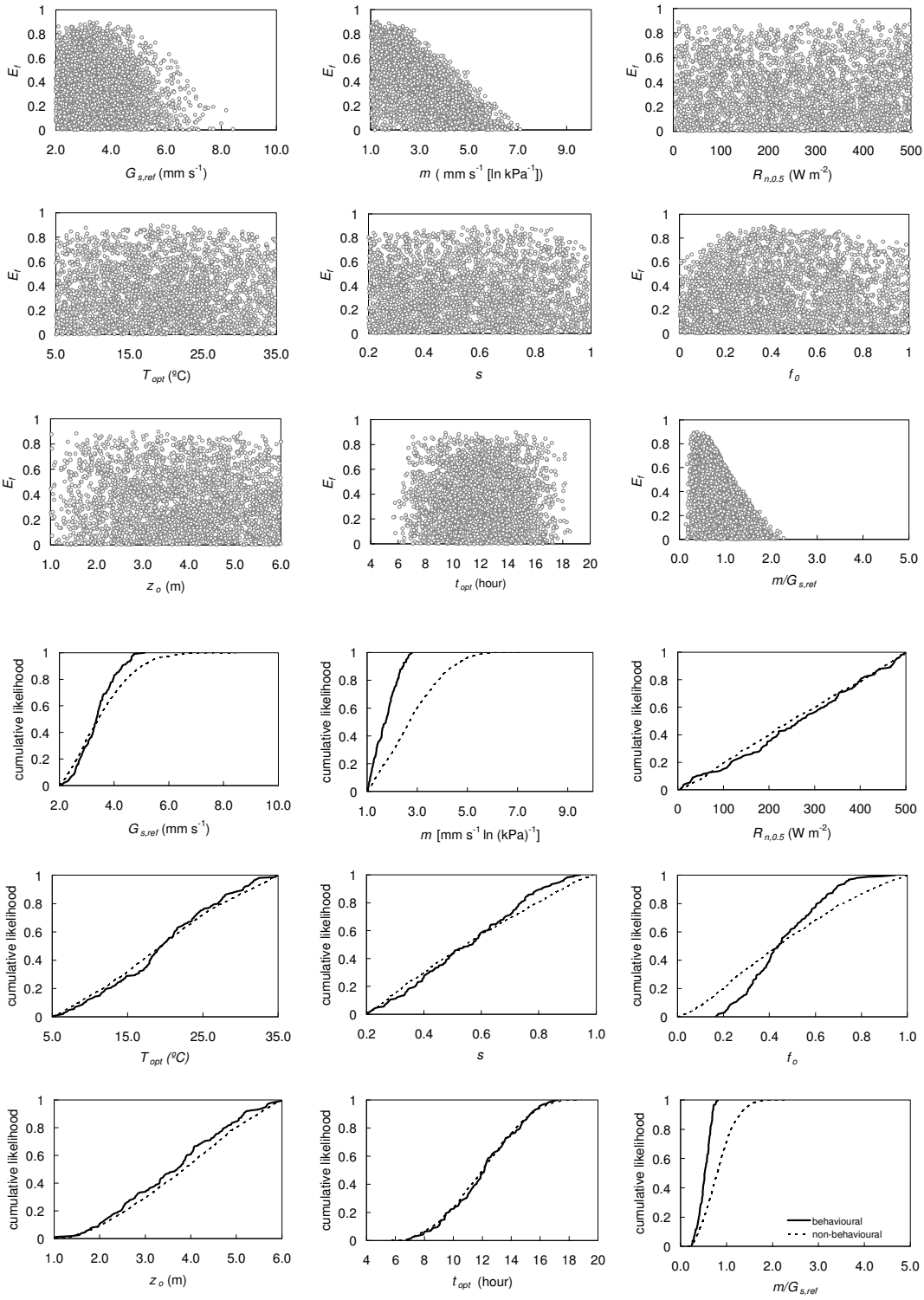

Figure 8. Parameter conditioning of the evapotranspiration model with sap flow data from year 2003 after 30,000 Monte Carlo realisations. (a) Plot of daily efficiency against parameter values included in the GLUE analysis (Table 3). Only simulations with E_f >0 are shown. (b) Cumulative likelihood distribution of the parameters, for behavioural (E_f>0.75) and non-behavioural models (E_f<0.75).

GLUE analysis: predictive uncertainty

The uncertainty bounds calculated solely on the basis of behavioural models for the 2004 calibration period, encompassed much of the data during 2003 and 2004, although the width of the bounds was very large for the 2003 dry summer (Fig. 1a). When validating against data from the year 2005 (validation), most of the observations fell out of the 5% and 95% uncertainty envelope or were close to the inferior 5% limit (Fig. 11a). This envelope was narrower when calculated with likelihoods conditioned on 2003 data, but then observations during the 2004 period lied closer to the superior limit instead of being centered around the uncertainty limits (Fig. 11b).

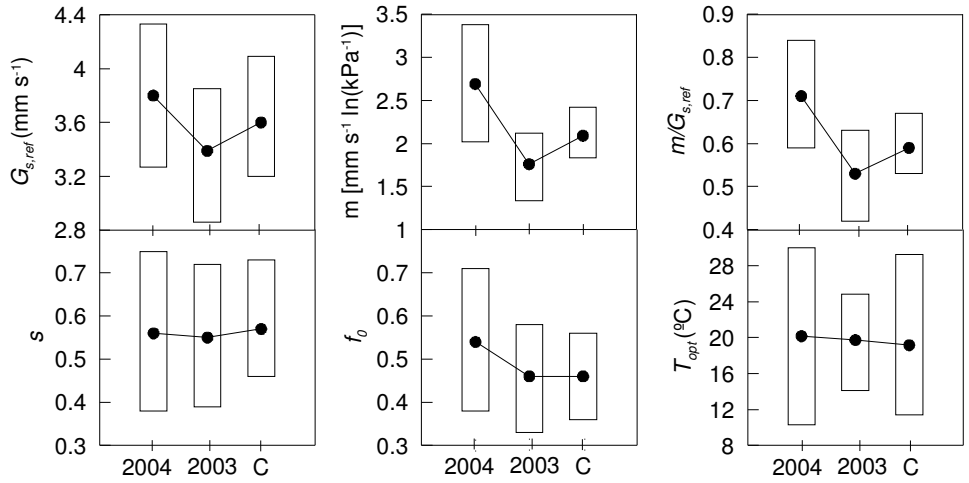

Figure. 9. Average value (dots) and interquartilic range (bars) of selected parameters for behavioural models when the model was constrained with 2004 data, 2003 data and the obtained likelihoods from both GLUE analysis were combined (C) as described in the text.

When the initial parameter conditioning on 2004 data was used as prior information and likelihoods were updated according to new likelihoods resulting from conditioning on the 2003 period, only 44 parameter sets were retained. Uncertainty bounds calculated on the basis of these parameter sets (Fig. 11c), were very similar to the ones obtained only from behavioural models of the 2003 period. We also represented an example of the uncertainty envelopes for 15-min data based on daily likelihood values for the initial calibration period (2004) (Fig. 12a) and the resulting updated likelihood weights (Fig. 12b), showing the narrower uncertainty envelopes with updated likelihoods. Therefore, although updating likelihoods with more calibration data has been shown to reduce predictive uncertainty in E_c estimates, there continues to be a poor performance of the model during 2005 (Figs. 10, 11) even when information from two distinct periods are incorporated in the calibration procedure.

Table 5. Performance of the model in terms of $E_c$calibrated using the boundary-line technique or using the best parameter set from the GLUE analysis. Number of observations (*N*), slope, intercept and coefficient of determination (R^2) of the linear regression between observed and simulated values for different periods at the instantaneous and daily time scales.

	Boundary-line parameterised					Best parameter set GLUE 2004			
	N	R^2	Slope	Intercept	E_f	R^2	Slope	Intercept	E_f
15-min									
2003	5010	0.72	1.15	4.80E-06	0.23	0.69	0.77	1.30E-05	0.49
2004	11091	0.67	1.05	1.20E-06	0.42	0.65	0.64	1.13E-05	0.65
2005	5968	0.49	1.08	1.70E-05	-1.35	0.52	0.71	2.00E-05	-0.18
Daily									
2003	151	0.85	0.98	0.250	0.38	0.86	1.34	0.002	0.43
2004	323	0.85	0.72	0.140	0.64	0.82	1.18	0.097	0.81
2005	160	0.75	0.96	0.500	-1.23	0.69	0.49	0.109	-0.18

4. Discussion

Forest floor micrometeorology and soil evaporation

Our simple representation of radiative transfer and soil heat flux did not allow for a precise simulation of understorey fluxes. However, the use of the Lambert-Beer law did not preclude the obtention of appropiate descriptions of diurnal dynamics of net radiation at the forest floor (Fig. 1). The observed κ for net radiation was larger than the values reported elsewhere for other canopy types (Kustas and Norman 1999). The multiple regression approach employed to derive *G* reproduced correctly the influence of soil moisture and the lag between radiative input and soil heat flux (Kustas and Norman 1999), but the fine resolution simulation of *G* requires more precise estimations of $R_{n,s}$.

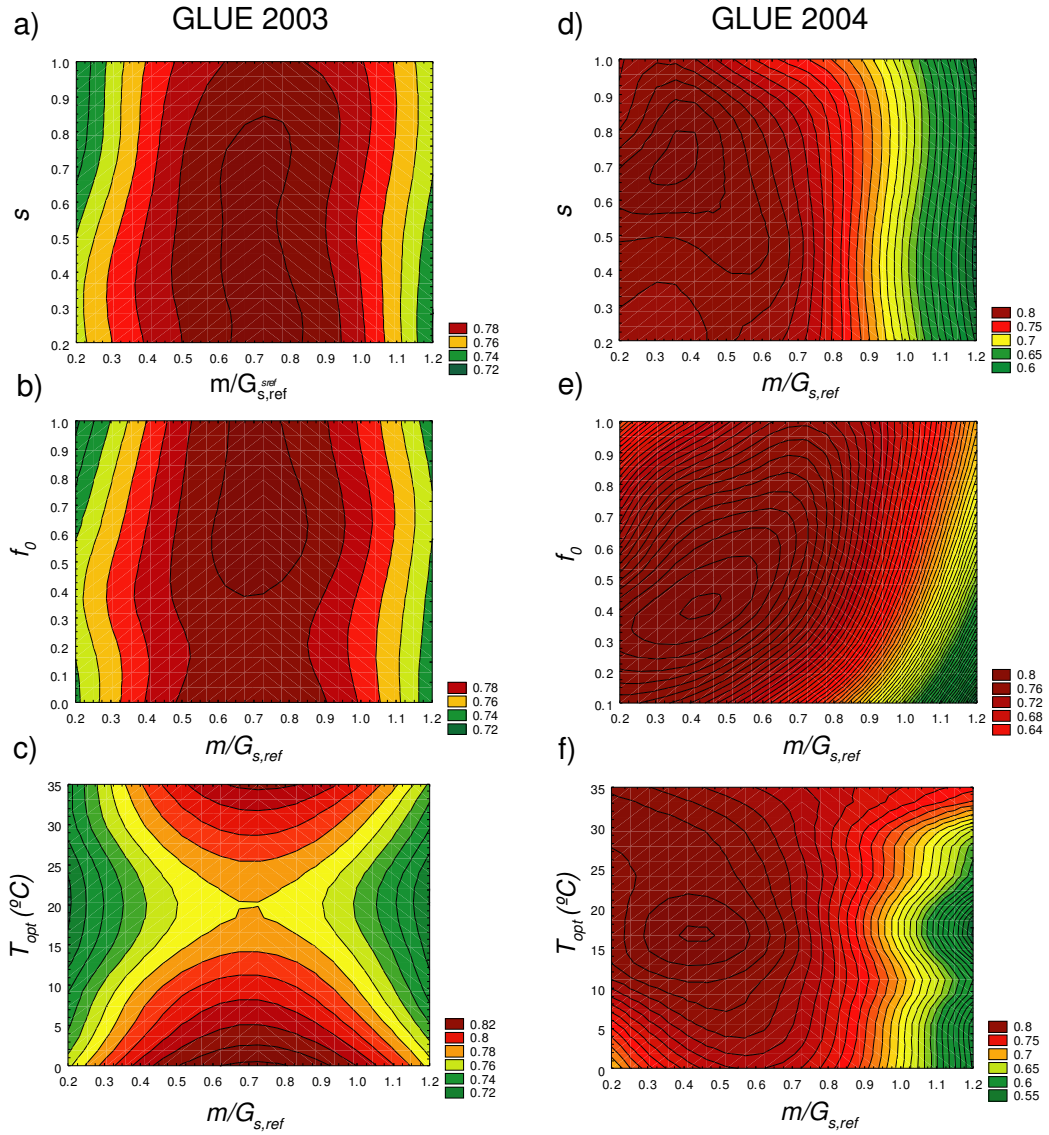

Figure. 10. Values of model efficiency of behavioural models conditioned on 2004 data (left column) and 2003 data (right column) related to the values of pairs of parameters in the G_s model.

Measured soil evaporation during 2005 was very low as a result of the low soil moisture content in the topsoil layers. However, the obtained function of soil surface resistance, similar in overall shape to other formulations found in the literature (Domingo et al. 1999; Wallace 1995), resulted in typical maximum values of E_s when the soil was wet, close to those found by Wilson et al. (2000). Similarly, soil evaporation rates in a Douglas-fir stand also increased from 0.2 to 0.4 mm day^{-1} when soil moisture conditions changed from dry to wet (Schaap and Bouten 1997).

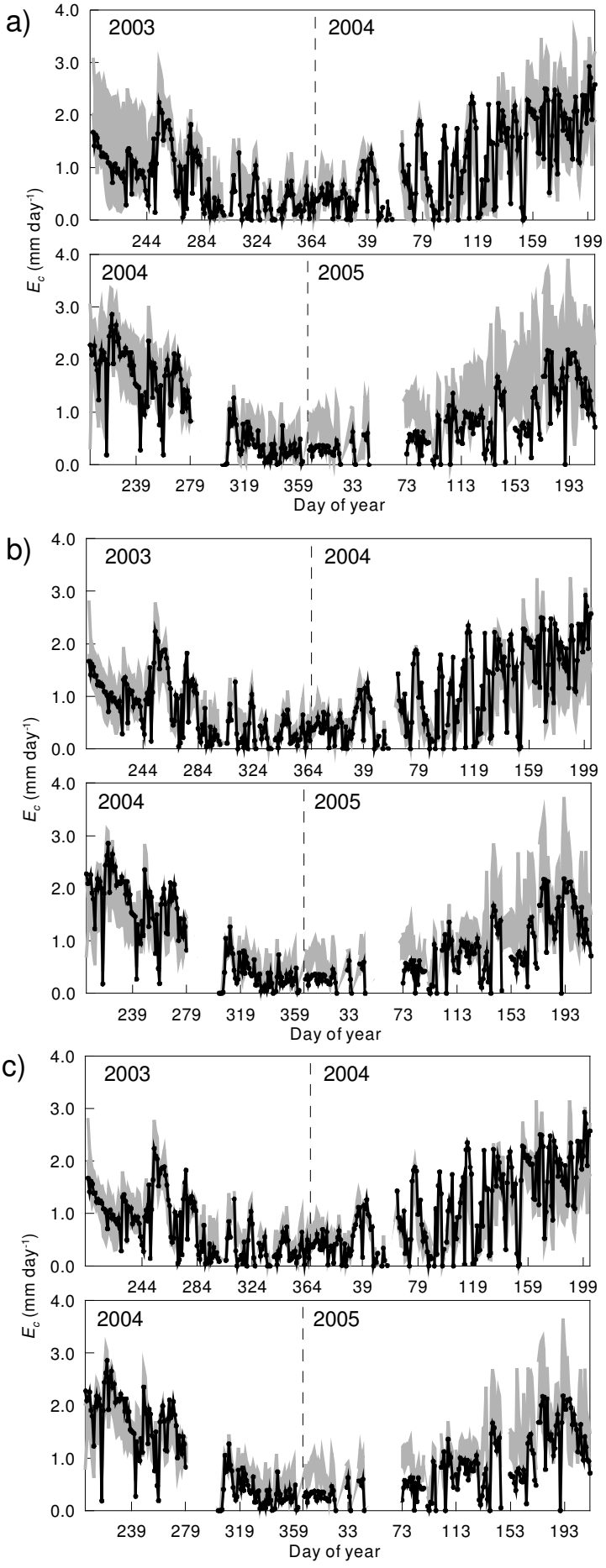

Figure 11. Uncertainty bounds (5% and 95%) of daily transpiration (E_c) (shaded area) in relation with observed E_c (black line). (a) For behavioural models when conditioned on 2004 data, (b) for behavioural models when conditioned on 2003 data and c)for sets retained after updating 2004 likelihoods with 2003 data.

Boundary-line parametrisation of canopy stomatal conductance and model performance

We suceeded in calibrating a Jarvis-type G_s model using a sequential parameterisation procedure based on boundary-line relationships (Granier et al. 2000; Lagergren and Lindroth 2002). The general shape of the functions was in accordance with previous findings on these species (Stewart 1988), with the addition of a function introducing variation due to time of day. This dependence on time has been reported in other studies (Huntingford and Cox 1997; Uddling et al. 2005), and been attributed to circadian rythms (Mencuccini et al. 2000) or responses to leaf water potential (Dolman and Burg 1988).

Although overall good fits were obtained with the boundary-line parameterisation for daily E_c during 2003 and 2004 (calibration dataset), the model did not simulate adequately 2005 data. Despite acceptable model performance for daily data in 2003 and 2004, the diurnal courses of modelled E_c significantly departed from the observations under certain environmental conditions. The model considerably overestimated E_c when soil moisture deficit was not limiting and extremely high D_r's also caused the model to reduce G_s excessively, leading to underestimation of E_c. One could argue that the soil moisture deficit function was arbitrarily assigned based on previous knowledge, and only checked visually against data. Several tests of alternative functions for *f(D)* and *f(*$SMD_{0\text{-}30}$*)* were carried out, but results did not significantly improve overall model performance.

Apart from the issue of finding the appropiate constraint functions, other unaccounted factors might be limiting model performace under the wide range of environmental conditions included in this study. Severe physiological changes must have taken place in the year 2005 to explain the poor performance of the model during this period. This will be further discussed in the next sections. Furthermore, multiplicative models bear additional problems concerning interactions and compensation among parameters (Fig. 9), due the inevitable correlation among some of the input variables (mainly T, R_n and D). Given the complexity of the issues exposed (parameter search, assessment of model structure and parameter interactions), we used the GLUE methodology to explore them further.

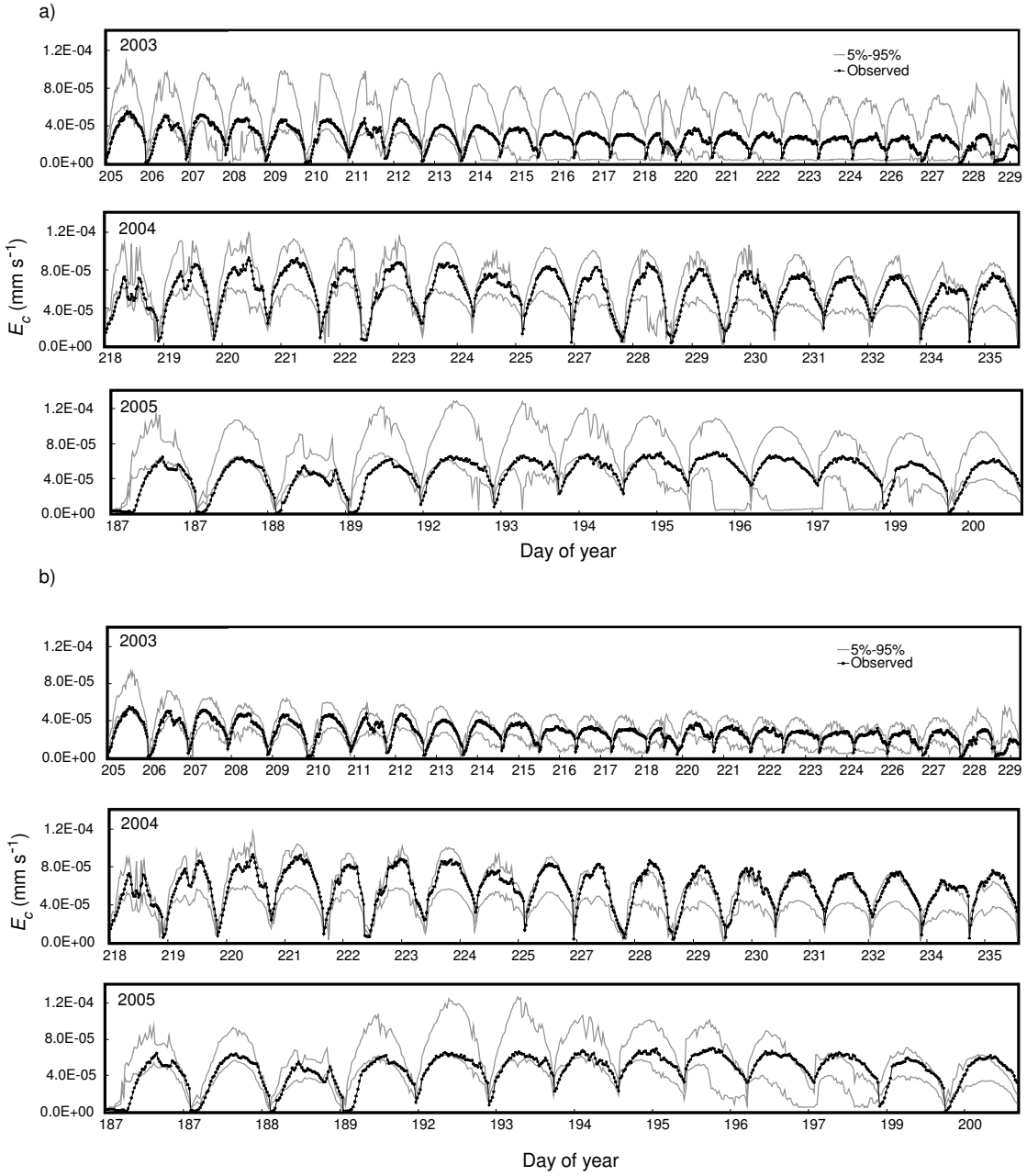

Figure 12. Uncertainty bounds (5% and 95%) for instantaneous E_c rates based on behavioural simulations using daily likelihoods for the three periods in Fig. 4. (a) Bounds based on behavioural simulations for the model conditioned on 2004 data and (b) posterior likelihoods after updating with 2003 data (see text for details). Observations are also shown.

Parameter space in the G_s model

Before discussing the issues regarding model behaviour, we will first acknowledge that Monte Carlo sampling of the parameter space yielded parameter sets with better overall efficiencies than the boundary-line analysis calibration (Table 5), despite not representing

the envelope functions as proposed in the original model formulation (Jarvis 1976). For the case of radiation, for example, the respective function in the model does not reach a maximum value of 1. Although leaf level stomatal conductance saturates at a certain value of irradiance (Ng and Jarvis 1980), when dealing with entire trees and canopies, higher irradiance means that more leaves open their stomata, contributing to increase G_s (Martin et al. 1997). The high correlation between D and T can also lead to mutual compensation between $G_{s,max}(D)$ and $f_3(T)$ (Ogink-Hendriks 1995). Mutual compensation between functions or the absence of other relevant factors in the G_s model may be responsible for these relationships not being truly envelopes.

Parameter conditioning on 2004 and 2003 data revealed that some information was missing on the behaviour of the system in the 2004 data set. When using these data for calibration, parameters controlling the soil moisture response of G_s appeared insensitive.

Moreover, the T_{opt} parameter was constrained on values in the extreme of the temperature range, in clear disagreement with usual reports of this temperature optimum for *P.sylvestris* (Beadle et al. 1985; Stewart 1988). When the model was calibrated with 2003 data, however, both parameters in $f_3(SMD_{0\text{-}30})$ became sensitive, specially f_0, and T_{opt} lied preferentially between 15 and 20 ºC.

The reason why the model was sensitive to soil moisture parameters only when calibrated against 2003 data, can be explained because although a wide range of $SMD_{0\text{-}30}$ conditions existed in 2004 (Chapter 4), the summer drought of 2003 was longer and more intense. This fact suggests that a lengthy dry period is necessary to detect G_s sensitivity to soil moisture parameters. It may also point at the need for including the influence of the whole soil profile on physiological regulation of G_s, not only the upper 30 cm, although some studies show that tree response to drought is closely related to moisture availability in the first centimeters of the soil, where fine root density is highest (Warren et al. 2005). The use of internally stored water in sapwood tissues to meet evaporative demand could also allow for G_s to remain open, decoupling stomatal dynamics from the increase in soil moisture deficits (Meinzer 2002).

Even though model residuals were not related to $SMD_{30\text{-}60}$, the f_0 parameter, representing the fraction of G_s remaining after $SMD_{0\text{-}30}$=1 showed a lower range when the model was conditioned on 2003 data (Table 5). A lower f_0 means a stronger reduction of G_s when there is no water availability in the upper soil, which might be linked to more depleted water reserves in deeper soil layers during 2003 (Rubio, unpublished data).

The average value of $G_{s,ref}$ for the behavioural models was 12% lower when the model was conditioned on 2003 data, while the reduction in m was higher (35%). This resulted in a decline in $m/G_{s,ref}$, and therefore, during the dry period, trees did not show an enhanced sensitivity of G_s to D (see Chapter 5). There is a noticeable similarity between the obtained

$m/G_{s,ref}$ and the theoretical slope between $G_{s,ref}$ and $G_{s,ref}$ ($dG_s/d\ln D \approx 0.6$) predicted by a hydraulic model assuming stomatal control of water potential to avoid cavitation and corroborated against an extensive survey of leaf and canopy-level observations (Oren et al. 1999). Recent studies have shown the consistency of Jarvis-type model of G_s with hydraulic theory (Mackay et al. 2003a), although they still recognise the influence of parameter compensation (Mackay et al. 2003b).

Limitations of Jarvis-type stomatal conductance models

Jarvis-type G_s models are attractive because of their simplicity and the relatively good results in predicting transpiration fluxes from forest canopies. For this reason, they have been widely incorporated into terrestrial biosphere models (Mackay et al. 2003a) and land-surface exchange schemes (Bartlett et al. 2003). Nevertheless, in very few occasions have this kind of models been tested again data comprising more than one growing season (but see Lagergren and Lindroth (2002)) and including such variable conditions as shown in this study. Model performance at the daily scale was relatively good during the years 2004 (calibration period) and 2003, but failed to simulate adequately E_c for the year 2005. In addition, the simulation of diurnal courses of E_c was not satisfactory under certain environmental conditions.

Using the GLUE methodology we explored the predictive uncertainty of the evapotranspiration model, and concluded that, even when we included additional data from a dry period to calibrate the model, it continued to overestimate E_c during 2005. Therefore, the current model structure could not account for the physiological processes regulating year-round E_c in the studied stand.

Stomatal conductance has been shown to be tightly linked to hydraulic conductance of the soil-to-leaf pathway (Irvine et al. 1998; Meinzer and Grantz 1990) which in turn can be reduced by drought-induced (Tyree and Sperry 1988) or freeze-thaw embolisms (Sperry and Sullivan 1992). Both situations must have surely arisen during the study period, which included an acute summer drought (summer 2003), and an extense dry period between autumn 2004 and spring 2005, which included some days of extremely low temperatures (see Chapter 5). This drought during a period when soil moisture is usually recovered from summer water deficits, is extremely unusual and might have been responsible for the mortality of Scots pine individuals in locations close to the study area, but at lower elevations, at the end of the spring 2005 (personal observation). In addition, the no consideration of capacitances in the trunk, may have precluded the correct simulation of diurnal courses of E_c when water stored in sapwood is being used to meet evaporative demand (Phillips et al. 1997). Recent comparisons among different G_s modelling schemes,

showed that coupled models and more physically-based approaches with less calibration effort may produce better results than the Jarvis multiplicative model (Falge 2005; Misson et al. 2004).

Why a two-layer model ?

Two-source evapotranspiration models based on the principles by Shuttleworth and Wallace (1985), applied to forest ecosystems, usually show superior performance than single-layer models, especially under wetter conditions when the contribution from the soil is highest (Fisher et al. 2005). This model encloses in a simple formulation, a physically sound description of within canopy processes, allowing interaction between fluxes from different surfaces and making the model very versatile to apply in forest with different densities, cover fractions and LAI (Daamen and McNaughton 2000).
However, we only validated the model against the canopy component of evapotranspiration and we could not test the validity of the model to simulate whole forest evapotranspiration. With whole surface vapour exchange (eddy covariance methods) or continuous E_s measurements (automatic lysimeters, within-canopy eddy covariance) the model could be further assessed, using the framework of the GLUE methodology. This method would permit a more robust model evaluation against multiple model outputs, as previously done for similar multi-source models predicting water and CO_2 fluxes (Mo and Beven 2004) .
Finally, an important shortcoming of our particular formulation of the physiological regulation of plant transpiration is its dependence on soil moisture as an input variable. This fact limits model applicability in hydrology, as this variable is unavailable from standard meteorological stations, and the model would be greatly improved by the inclusion of a soil water balance subroutine. More realistic descriptions of plant and soil resistances and how they vary with evaporative demand and water supply (for example Williams et al. (2001), may also be included in these two-source evapotranspiration models to generalize their applicability across different stands and varying conditions.

Conclusions

We have shown how plant and soil controls on evaporation can be modelled within a two-source modelling framework using sap flow an soil evaporation measurements. The use of one-year sap flow data to calibrate the G_s submodel with quantile regression techniques yielded good fits at the daily level. However, this parameterisation technique was not superior to a stochastic Monte Carlo sampling of the parameter space.

Examination of diurnal courses also showed consistent E_c overestimations when soil moisture deficit was low. Modelled soil evaporation represented a small fraction of total evaporation during the growing season. The GLUE methodology showed that the parameters controlling reference stomatal aperture and sensitivity to *D* were the most relevant. Additional calibration with data including a long dry period was needed to detect substantial sensitivity of soil moisture parameters. This fact supports the view that Jarvis-type G_s models require extensive datasets to be tuned. Regardless of the calibration procedure, the model could not predict E_c adequately during the year 2005, pointing at the inadequacy of multiplicative G_s models to simulate physiological regulation of transpiration under the conditions of evaporative demand and soil moisture characteristic of Mediterranean mountain areas.

Appendix. Model structure

The energy budget for the whole surface under consideration can be expressed as

$$A = \lambda E + H = R_n - G \quad \text{(A1)}$$

Where *A* is available energy at the surface and *H* is sensible heat flux. In this formulation physical and biochemical energy storage components have been omitted. Similarly, the specific energy balance at the forest soil is given by

$$A_s = \lambda E_s + H_s = R_n{}^s - G \quad \text{(A2)}$$

According to the resistance network, vapour pressure deficit at the canopy source height D_0 is calculated as (Shuttleworth and Wallace, 1985)

$$D_0 = D + \{\Delta A - (\Delta + \gamma)\lambda E\} r_a{}^a / \rho c_p \quad \text{(A3)}$$

Where Δ is the slope of saturation vapour pressure curve against temperature, γ is the psychrometric constant, and λ is latent heat of vaporisation of water.

Then, evapotranspiration from the two sources can be expressed as a function of this D_0

$$\lambda E_s = (\Delta A_s + \rho c_p D_0 / r_a^s)\{\Delta + \gamma(1 + r_s^s / r_a^s)\}^{-1} \quad \text{(A4)}$$

$$\lambda E_c = \{(\Delta(A - A_s) + \rho c_p D_0 / r_a^c)\}\{\Delta + \gamma(1 + r_s^c / r_a^c)\}^{-1} \quad \text{(A5)}$$

Considering that

$$\lambda E = \lambda E_c + \lambda E_s \quad \text{(A6)}$$

And after some algebra manipulation (Shuttleworth and Wallace, 1985) we get

$$\lambda E = C_c PM_c + C_s PM_s \quad \text{(A7)}$$

Where *PM* terms are pseudo Penman Monteith combination equations:

$$PM_c = \frac{\Delta A_s + (\rho c_p D_r - \Delta r_a^c A_s)/(r_s^a / r_a^c)}{\Delta + \gamma[1 + r_s^c/(r_a^a + r_a^c)]} \quad \text{(A8)}$$

$$PM_s = \frac{\Delta A + [\rho c_p D_r - \Delta r_a^s (A - A_s)]/(r_a^a / r_a^s)}{\Delta + \gamma[1 + r_s^c/(r_a^a + r_a^c)]} \quad \text{(A9)}$$

And coefficients C_c and C_s result from the combination of resistances and thermodynamic parameters Δ and γ

$$C_c = [1 + R_c R_a / R_s (R_c + R_a)]^{-1} \quad \text{(A10)}$$

$$C_s = [1 + R_s R_a / R_c (R_s + R_a)]^{-1} \quad \text{(A11)}$$

Where

$$R_a = (\Delta + \gamma) r_a^a \quad \text{(A12)}$$

$$R_s = (\Delta + \gamma) r_a^s + \gamma r_s^s \quad \text{(A13)}$$

$$R_s = (\Delta + \gamma) r_a^c + \gamma r_s^c \quad \text{(A14)}$$

Equation A7 allows the calculation of A3, and in turn, the contribution of each source to total evapotranspiration is obtained with equations A4 and A5. The calculations begin using D_r instead of D_0, then D_0 is calculated using equation A3. An iterative process begins until the difference between consecutive D_0 values is less than 0.005 kPa.

References

Bartlett, P.A., J.H. McCaughey, P.M. Lafleur and D.L. Verseghy 2003. Modelling evapotranspiration at three boreal forest stands using the class: Tests of parameterizations for canopy conductance and soil evaporation. International Journal of Climatology. 23:427-451.

Beadle, C.L., R.E. Neilson, H. Talbot and P.G. Jarvis 1985. Stomatal conductance and photosynthesis in a mature Scots Pine forest. II. Dependence on environmental variables of single shoots. J Appl Ecol. 22:573-586.

Beadle, C.L., H. Talbot and P.G. Jarvis 1982. Canopy structure and leaf area index in a mature Scots pine forest. Forestry. 55:105-127.

Bernhofer, C., J.H. Blandford, R. Siegwolf and M.Wedler 1996. Applying single and two layer canopy models to derive conductances of a Scots pine plantation from micrometeorological measurements. Theoretical and Applied Meteorology. 53:95-104.

Beven, K. and A. Binley 1992. The future of distributed models: model calibration and uncertainty prediction. Hydrological Processes. 6:279-298.

Beven, K. and J. Freer 2001. Equifinality, data assimilation, and uncertainty estimation in mechanistic modelling of complex environmental systems using the GLUE methodology. J Hydrol. 249:11-29.

Brenner, A.J. and L.D. Incoll 1997. The effect of clumping and stomatal response on evaporation from sparsely vegetated shrublands. Agric For Meteorol. 84:187-205.

Camillo, P.J. and R.J. Gurney 1986. A resistance parameter for bare soil evaporation models. Soil Sci. 141:95-105.

Chambers, J.L., T.M.Hinckley, G.S. Cox, C.L. Metcalf and R.G. Aslin 1985. Boundary-Line Analysis and Models of Leaf Conductance for Four Oak-Hickory Forest Species. For Sci. 31:437-450.

Daamen, C.C. and K.G. McNaughton 2000. Modeling energy fluxes from sparse canopies and understorys. Agron J. 92:837-847.

Daamen, C.C., L.P. Simmonds, J.S. Wallace, K.B. Laryea and M.V.K. Sivakumar 1993. Use of microlysimeters to measure evaporation from sandy soils. Agric For Meteorol. 65:159-173.

Dolman, A.J. and G.J.V.D. Burg 1988. Stomatal behaviour in an oak canopy. Agric For Meteorol. 43:99-108.

Domingo, F., L. Villagarcía, A.J. Brenner and J. Puigdefábregas 1999. Evapotranspiration model for semi-arid shrub-lands teste against data from SE Spain. Agric For Meteorol. 95:67-84.

Ewers, B.E. and R. Oren 2000. Analyses of assumptions and errors in the calculation of stomatal conductance from sap flux measurements. Tree Physiol. 20:579-589.

Falge, E. 2005. Comparison of surface energy exchange models with eddy flux data in forest and grassland ecosystems of Germany. Ecol Model. 188:174-216.

Fisher, J.B., T.A. DeBiase, Y. Qi, M. Xu and A.H. Goldstein 2005. Evapotranspiration models compared on a Sierra Nevada forest ecosystem. Environmental Modelling & Software. 20:783-896.

Franks, S.W. and K.J. Beven 1997. Bayesian estimation of uncertainty in land surface-atmosphere flux predictions. Journal of Geophysical Research D: Atmospheres. 102:23991.

Franks, S.W., K.J. Beven, P.F. Quinn and I.R. Wright 1997. On the sensitivity of soil-vegetation-atmosphere transfer (SVAT) schemes: Equifinality and the problem of robust calibration. Agric For Meteorol. 86:63.

Gallart, F., P. Llorens, J. Latron and D. Regüés 2002. Hydrological processes and their seasonal controls in a small Mediterranean mountain catchment in the Pyrenees. Hydrol Earth Syst Sci. 6:527-537.

Granier, A. 1985. Une nouvelle méthode pur la mesure du flux de sève brute dans le tronc des arbres. Ann Sci For. 42:193-200.

Granier, A., P. Biron, B. Köstner, L.W. Gay and G. Najjar 1996. Comparisons of xylem sap flow and water vapour flux at the stand level and derivation of canopy conductance for Scots Pine. Theor Appl Clim. 53:115-122.

Granier, A., P. Biron and D. Lemoine 2000. Water balance, transpiration and canopy conductance in two beech stands. Agric For Meteorol. 100:291-308.

Granier, A. and D. Loustau 1994. Measuring and modelling the transpiration of a maritime pine canopy from sap-flow data. Agric For Meteorol. 71:61-81.

Hanson, P.J. 2004. Oak forest carbon and water simulations:model intercomparisons and evaluation against independent data. Ecol Monogr. 74:443-489.

Huntingford, C., S.J. Allen and R.J. Harding 1995. An Intercomparsion of Single and Dual-Source Vegetation-Atmosphere Transfer Models Applied to Transpiration from Sahelian Savannah. Boundary-Layer Meteorology. 74:397-418.

Huntingford, C. and P.M. Cox 1997. Use of statistical and neural network techniques to detect how stomatal conductance responds to changes in the local environment. Ecol Model. 97:217-246.

Iritz, Z., A. Lindroth, M. Heikinheimo, A. Grelle and E. Kellner 1999. Test of a modified Shuttleworth-Wallace estimate of boreal forest evaporation. Agric For Meteorol. 98-99:605-619.

Irvine, J., M.P. Perks, F. Magnani and J. Grace 1998. The response of *Pinus sylvestris* to drought: stomatal control of transpiration and hydraulic conductance. Tree Physiol. 18:393-402.

Jarvis, P.G. 1976. The interpretation of the variations in leaf water potential and stomatal conductance found in canopies in the field. Philos Trans R Soc Lond B Biol Sci. 273:593-610.

Kustas, W.P. and J.M. Norman 1999. Evaluation of soil and vegetation heat flux predictions using a simple two-source model with radiometric temperatures for partial canopy cover. Agric For Meteorol. 94:13-29.

Lagergren, F. and A. Lindroth 2002. Transpiration response to soil moisture in pine and spruce trees in Sweden. Agric For Meteorol. 112:67-85.

Leuning, R. 1995. A critical appraisal of a combined stomatal-photosynthesis model for C3 plants. Plant, Cell and Environment. 18:339-355.

Llorens, P. and F. Gallart 2000. A simplified method for forest water storage capacity measurement. J Hydrol. 240:131.

Mackay, D.S., D.E. Ahl, B.E. Ewers, S. Samanta, S.T. Gower and S.N. Burrows 2003a. Physiological tradeoffs in the parameterization of a model of canopy transpiration. Advances in Water Resources. 26:179-194.

Mackay, D.S., S. Samanta, R.R. Nemani and L.E. Band 2003b. Multi-objective parameter estimation for simulating canopy transpiration in forested watersheds. J Hydrol. 277:230-247.

Martin, T.A., K.J. Brown, J. Čermák, R. Ceulemans, J. Kučera, F.C. Meinzer, J.S. Rombold, D.G. Sprugel and T.M. Hinckley 1997. Crown conductance and tree and stand transpiration in a second-growth Abies amabilis forest. Can J For Res. 27:797-808.

Massman, W.J. 1992. Correcting errors associated with soil heat flux measurements and estimating soil thermal properties from soil temperature and heat flux plate data. Agricultural & Forest Meteorology. 59:249.

McNaughton, K.G. and P.G. Jarvis 1991. Effects of spatial scale on stomatal control of transpiration. Agric For Meteorol. 54:279-301.

Meinzer, F.C. 2002. Co-ordination of vapour and liquid phase water transport properties in plants. Plant Cell Environ. 25:265-274.

Meinzer, F.C. and D.A. Grantz 1990. Stomatal and hydraulic conductance in growing sugarcane -stomatal adjustmentto water transport capacity. Plant Cell Environ. 13:383-388.

Mencuccini, M., S. Mambelli and J. Comstock 2000. Stomatal responsiveness to leaf water status in common bean (Phaseolus vulgaris L.) is a function of time of day. Plant, Cell and Environment. 23:1109-1118.

Misson, L., J.A. Panek and A.H. Goldstein 2004. A comparison of three approaches to modeling leaf gas exchange in annually drought-stressed ponderosa pine forests. Tree Physiol. 24:529.

Mo, X. and K. Beven 2004. Multi-objective parameter conditioning of a three-source wheat canopy model. Agric For Meteorol. 122:39-63.

Monteith, J.L. 1965. Evaporation and environment. Symposia of the Society for Experimental Biology. 19:205-234.

Nash, J.E. and J.V. Sutcliffe 1970. River flow forecasting through conceptual models: Part I - A discussion of principles. J Hydrol. 10:282.

Ng, P.A.P. and P.G. Jarvis 1980. Hystereis in the response of stomatal conductance in Pinus sylvestris L. needles to light: observations and a hypothesis. Plant Cell Environ. 3:207-216.

Ogink-Hendriks, M.J. 1995. Modelling surface conductance and transpiration of an oak forest in The Netherlands. Agric For Meteorol. 74:99-118.

Oren, R., J.S. Sperry, G.G. Katul, D.E. Pataki, B.E. Ewers, N. Phillips and K.V.R. Schafer 1999. Survey and synthesis of intra- and interspecific variation in stomatal sensitivity to vapour pressure deficit. Plant Cell Environ. 22:1515-1526.

Phillips, N., A. Nagchaudhuri, R.Oren and G.Katul 1997. Time constant for water transport in Loblolly pine trees estimated from time series of evaporative demand and stem sapflow. Trees. 11:412-419.

Poyatos, R., J. Latron and P. Llorens 2003. Land-use and land cover change after agricultural abandonment. The case of a Mediterranean Mountain Area (Catalan Pyrenees). Mt Res Dev. 23:52-58.

Poyatos, R., P. Llorens and F. Gallart 2005. Transpiration of montane *Pinus sylvestris* L. and *Quercus pubescens* Willd. forest stands measured with sap flow sensors in NE Spain. Hydrol Earth Syst Sci. 9:493-505.

Raupach, M.R. and J.J. Finnigan 1988. 'Single-layer Models of Evaporation from Plant Canopies are incorrect but useful, Whereas Multilayer Models are Correct but Useless': Discuss. Aust J Plant Physiol. 15:705-716.

Schaap, M.G. and W. Bouten 1997. Forest floor evaporation in a dense Douglas fir stand. J Hydrol. 193:97-113.

Shuttleworth, W.J. and R.J. Gurney 1990. The theoretical relationship beween foliage temperature and canpoy resistance in sparse crops. Quarterly Journal of the Royal Meteorological Society. 116:497-519.

Shuttleworth, W.J. and J.S. Wallace 1985. Evaporation from sparse crops- an energy combination theory. Quarterly Journal of the Royal Meteorological Society. 111:839-855.

Sperry, J.S. and J.E.M. Sullivan 1992. Xylem embolism in response to freeze-thaw cycles and water stress in ring-porous, diffuse-porous,and conifer species. Plant Physiology. 100:605-613.

Stewart, J.B. 1988. Modelling surface conductance of pine forest. Agric For Meteorol. 43:19-35.

Tyree, M.T. and J.S. Sperry 1988. Do woody plants operate near the point of catastrophic xylem dysfunction by dynamic water stress? Plant Physiology. 88:574-580.

Uddling, J., M. Hall, G. Wallin and P.E. Karlsson 2005. Measuring and modelling stomatal conductance and photosynthesis in mature birch in Sweden. Agric For Meteorol. 132:115-131.

Wallace, J.S. 1995. Calculating evaporation: resistance to factors. Agricultural & Forest Meteorology. 73:353-366.

Warren, J.M., F.C. Meinzer, J.R. Brooks and J.C. Domec 2005. Vertical stratification of soil water storage and release dynamics in Pacific Northwest coniferous forests. Agric For Meteorol. 130:39-58.

Whitehead, D. and P.G. Jarvis 1981. Coniferous forests and plantations. *In* Water Deficits and Plant Growth Ed. T.T. Kozlowski. Academic Press, New York, pp. 49-152.

Williams, M., B.J. Bond and M.G. Ryan 2001. Evaluating different soil and plant hydraulic constraints on tree function using a model and sap flow data from ponderosa pine. Plant Cell Environ. 24:679-690.

Wilson, K.B., P.J. Hanson and D.D. Baldocchi 2000. Factors controlling evaporation and energy partitioning beneath a deciduous forest over an annual cycle. Agric For Meteorol. 102:83-103.